Accepted Manuscript

Chiral 6-aryl-furo[2,3-*d*]pyrimidin-4-amines as EGFR inhibitors

Jin Han, Svein Jacob Kaspersen, Sondre Nervik, Kristin Nørsett, Eirik Sundby, Bård Helge Hoff

PII: S0223-5234(16)30347-6

DOI: 10.1016/j.ejmech.2016.04.054

Reference: EJMECH 8569

To appear in: *European Journal of Medicinal Chemistry*

Received Date: 16 February 2016

Revised Date: 4 April 2016

Accepted Date: 22 April 2016

Please cite this article as: J. Han, S.J. Kaspersen, S. Nervik, K. Nørsett, E. Sundby, B.H. Hoff, Chiral 6-aryl-furo[2,3-*d*]pyrimidin-4-amines as EGFR inhibitors, *European Journal of Medicinal Chemistry* (2016), doi: 10.1016/j.ejmech.2016.04.054.

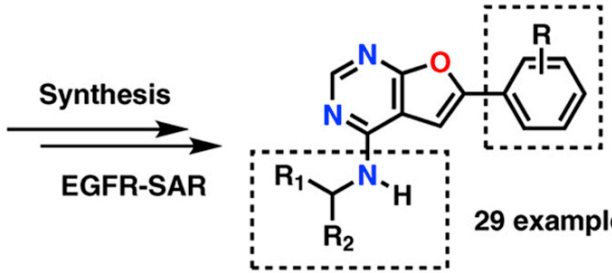

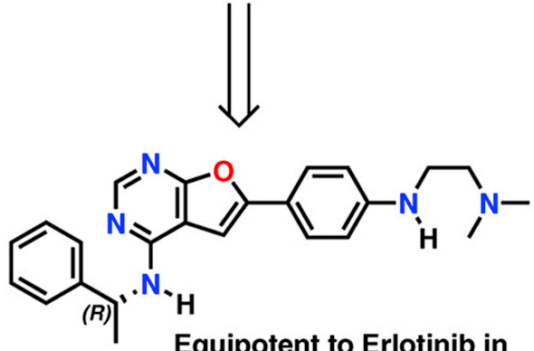

Equipotent to Erlotinib in enzymatic assay

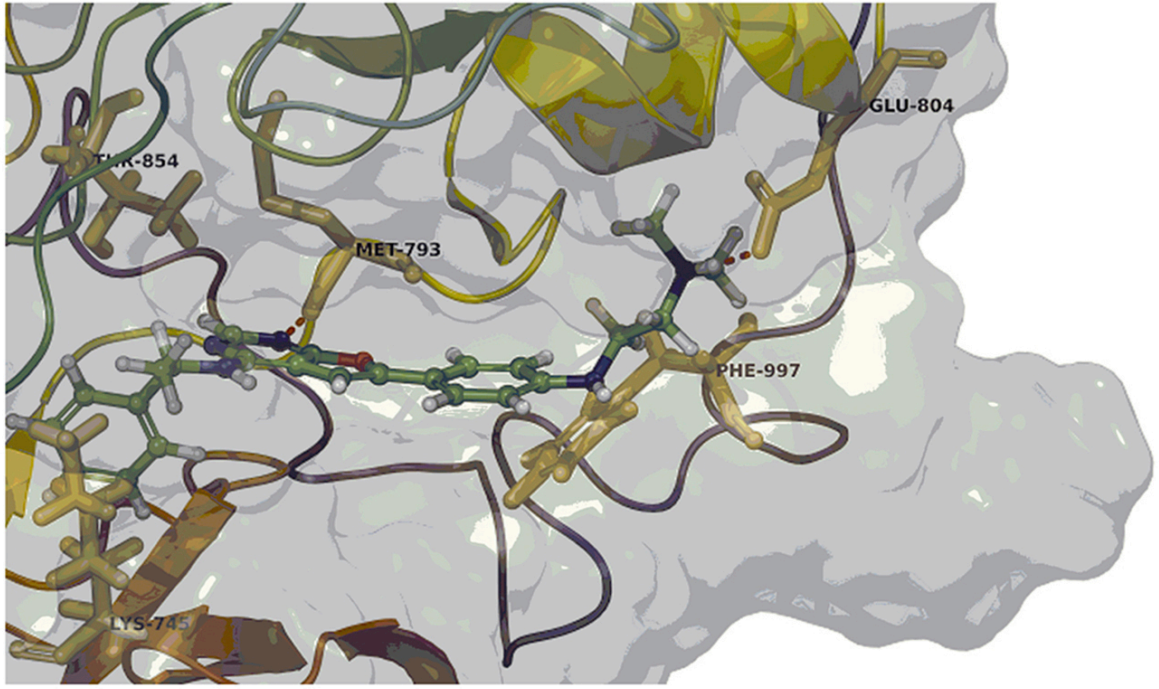

Title Page

Manuscript: Chiral 6-aryl-furo[2,3-*d*]pyrimidin-4-amines as EGFR inhibitors

Jin Han[a,b], Svein Jacob Kaspersen[a,c], Sondre Nervik[a], Kristin Nørsett[d], Eirik Sundby[b], Bård Helge Hoff[a]*

Adresses:

[a)]Norwegian University of Science and Technology, Department of Chemistry, Høgskoleringen 5, NO-7491 Trondheim, Norway.[b)] Norwegian University of Science and Technology, Institute of Chemistry and Material Technology, Faculty of Technology, NTNU, 7491 Trondheim. [c)] Current address: Jotun Marine and Protective Coatings, Rosenvoldsgt. 19, NO-3202 Sandefjord, Norway.[d)]Norwegian University of Science and Technology, Department of Cancer Research and Molecular Medicine, Prinsesse Kristinas gt. 1 N-7006 Trondheim, Norway.

Corresponding author:

** Bård H. Hoff, Department of Chemistry, Norwegian University of Science and Technology (NTNU), NO-7491, Norway. Email:* Bard.Helge.Hoff@chem.ntnu.no*, phone: ++004773593973, fax: ++004773594256.*

E-mail:
J. Han: Jin.Han@ntnu.no; S. J. Kaspersen: Svein.Jacob.Kaspersen@chem.ntnu.no; S. Nervik: Sondre.Nervik@ntnu.no; K. Nørsett: Kristin.Norsett@ntnu.no; E. Sundby: Eirik.Sundby@hist.no; B.H. Hoff: Bard.Helge.Hoff@chem.ntnu.no;

Chiral 6-aryl-furo[2,3-*d*]pyrimidin-4-amines as EGFR inhibitors

Jin Han[a,b], Svein Jacob Kaspersen[a,c], Sondre Nervik[a], Kristin Nørsett[d], Eirik Sundby[b], Bård Helge Hoff[a]*

[a)]Norwegian University of Science and Technology, Department of Chemistry, Høgskoleringen 5, NO-7491 Trondheim, Norway.[b)] Norwegian University of Science and Technology, Institute of Chemistry and Material Technology, Faculty of Technology, NTNU, 7491 Trondheim. [c)] Current address: Jotun Marine and Protective Coatings, Rosenvoldsgt. 19, NO-3202 Sandefjord, Norway.[d)]Norwegian University of Science and Technology, Department of Cancer Research and Molecular Medicine, Prinsesse Kristinas gt. 1 N-7006 Trondheim, Norway.

Corresponding author: ** Bård H. Hoff, Department of Chemistry, Norwegian University of Science and Technology (NTNU), NO-7491, Norway. Email:* Bard.Helge.Hoff@chem.ntnu.no*, phone: ++004773593973, fax: ++004773594256.*

Abstract: Epidermal growth factor receptor inhibitors are of importance in cancer therapy and possibly in the management of pain. Herein, we report a structure-activity relationship study with 29 new 6-aryl-furo[2,3-*d*]pyrimidin-4-amines, involving modification of the 4-amino group and 6-aryl function. The EGFR activity was especially dependent on having a chiral 4-benzylamino group with correct stereochemistry. Molecular dynamics indicate this to be due to favourable cation-π interactions. The most active inhibitor identified, equipotent to Erlotinib, was substituted with (*R*)-1-phenylethylamine at C-4 and a *N*',*N*'-dimethylethane-1,2-diamine group in *para* position of the 6-aryl moiety. These new furopyrimidines had a different off-target kinase profile when compared to Erlotinib, and also possessed high activity towards Ba/F3 $EGFR^{L858R}$ reporter cells. Further, comparing the EGFR data of the furo[2,3-*d*]pyrimidin-4-amines with that of the corresponding thieno- and pyrrolopyrimidines concludes the furopyrimidine scaffold to be highly useful for development of new epidermal growth factor receptor antagonists.

Keywords: Furopyrimidine; EGFR; Erlotinib; kinase, chiral drug

1 Introduction

Epidermal growth factor receptor (EGFR) signalling is important in the progression of several tumour types [1-4], and there is evidence that this receptor also can be targeted in pain treatment [5, 6]. Commercial small molecular EGFR inhibitors, examples including Erlotinib, Gefitinib and Lapatinib, are based on the quinazoline scaffold [7, 8], while investigational drugs containing thieno- [9, 10] and pyrrolopyrimidine [11-13] have also been reported. Possibly, due to the bad reputation of furans as inducers of toxic effects [14], kinase inhibitors based on furopyrimidines have been considerably less studied. However, some examples exist including: **I** a receptor interacting protein 1 (RIP1) kinase inhibitor [15], **II** a multikinase inhibitor [16], **III** an aurora kinase inhibitor [17], **IV** a dual vascular endothelial growth factor 2 (VEGF2) and angiopoietin-1 receptor kinase (Tie-2) inhibitor [18]. In

addition, Traxler found compound **V** to be a potent EGFR inhibitor [19], while Peng *et al.* developed **VI** indicated selective for the EGFR^{L858R} mutant [20], see Figure 1.

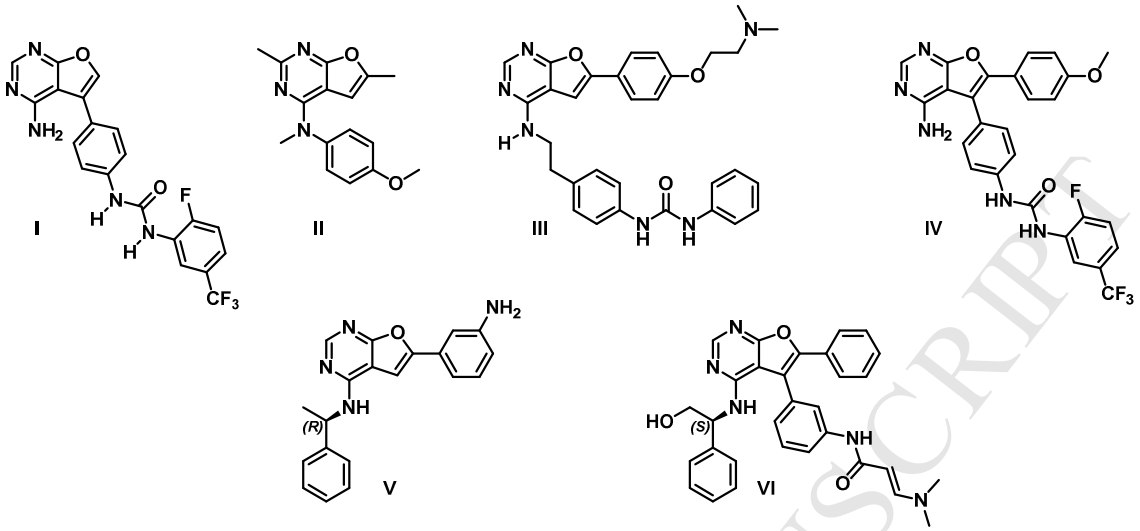

Figure 1. Examples of furopyrimidines previously evaluated as kinase inhibitors.

Herein we describe our structure-activity relationship (SAR) study and efforts towards potent 6-aryl-furo[2,3-*d*]pyrimidin-4-amines as EGFR inhibitors.

2 Result and Discussion

2.1 Design of the study

The main objective of the study was to identify new potent EGFR inhibitors based on the furopyrimidine scaffold. This was inspired by our previous work on thieno- [9, 10, 21] and pyrrolopyrimidines [13, 22, 23].

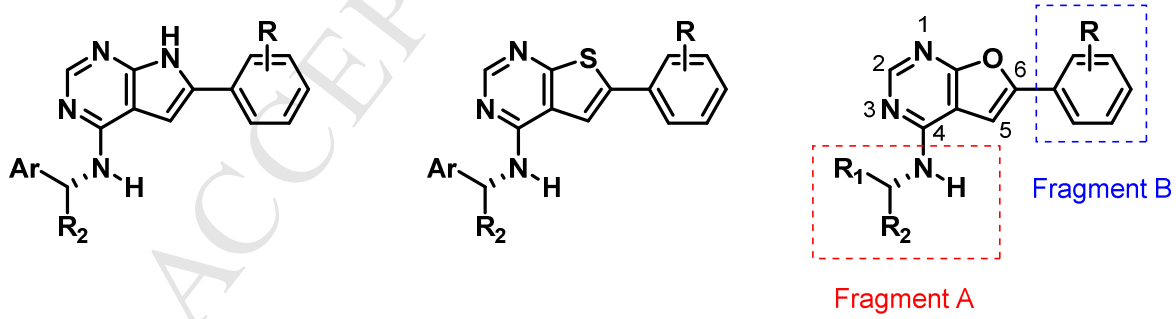

Figure 2. Structure of thieno-, pyrrolo- and the investigated furopyrimidines.

Compared to pyrrolopyrimidines, the furopyrimidines lack the N-H unit as presented by the pyrrole, and in this way the furopyrimidine is a closer bioisoster of the thienopyrimidine, see Figure 2. On the other hand, the size of the five-membered furan is more similar to the pyrrole than the thiophene. As both these related scaffolds have been applied for construction

of highly potent EGFR antagonists, we hypothesised that also the furopyrimidines should be useful in this setting. Fourteen variations of the 6-aryl group (Fragment B) were investigated. Eight derivatives were included for direct comparison with previous data in the thieno- and pyrrolopyrimidine series (*ortho*-, *meta*- and *para*-methoxy, *ortho*-, *meta*- and *para*-phenolic, *para*-fluorine and the unsubstituted analogue). Additionally, being structurally related to tyrosine, the phenolic derivatives might engage in a number of interactions [24], while the methoxy function is a moderately good hydrogen bond acceptor found useful in the corresponding thieno- and pyrrolopyrimidine analogues [10, 13]. The *para*-bromo and *para*-cyano compounds were mainly intended as precursor for other compounds. In the latter case, this was not viable due to the low yield in synthesis. In the 4-amino group (Fragment A) we included thirteen different variations. The selection was done both with the desire to yield potent inhibitors and to study protein-ligand interaction. Nine of these sub-structural elements have also been evaluated in the corresponding pyrrolopyrimidine series of compounds [13, 22].

2.2 Synthesis

The synthetic routes are outlined in Scheme 1 and 2. Starting with 1-aryl-2-bromoethanones **1**, the 2-amino-5-aryl-3-cyanofurans **3**, were made by a one-pot procedure using *N'*,*N'*-diethylamine as base. Addition of reagents was done at 0 °C, followed by 4.5 - 6 hours stirring at room temperature. The starting material was rapidly consumed and a build-up of intermediate **2** was seen by ^{1}H NMR spectroscopy. Work-up was done by quenching followed by washing with water resulting in mediocre yield and purity. No defined by-products were seen by ^{1}H NMR spectroscopy, indicating impurities to be of polymeric origin. Attempted further purification by silica-gel column chromatography or re-crystallisation resulted in decomposition and loss of material. A change in colour was noticed when the compounds were stored. Thus, we assume these furans to be unstable as indicated for similar compounds [25].

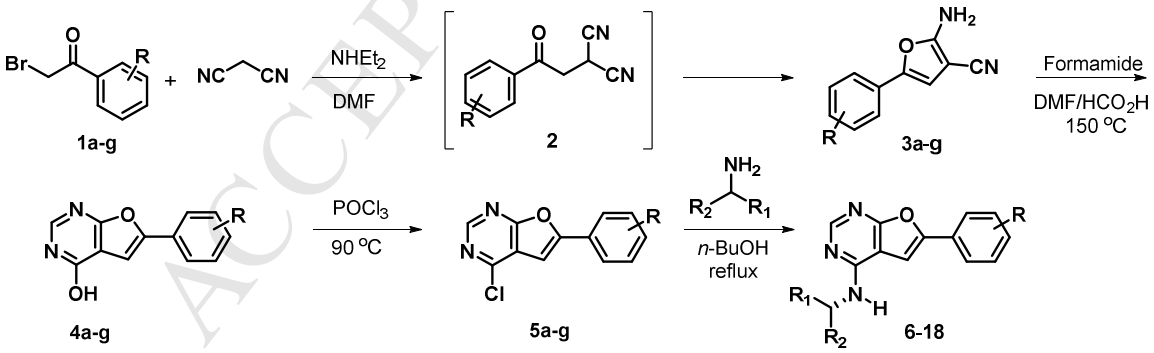

R = *p*-OMe (**a**), H (**b**), *p*-F (**c**), *p*-Br (**d**), *p*-CN (**e**), *m*-OMe (**f**), *o*-OMe (**g**).

R_1= Ph, R_2 = CH_3 (**6**), CH_2OH (**7**), H (**8**), CH_2OMe (**9**), Et (**10**), CH_2CONH_2 (**11**), CH_2CH_2OH (**12**).

R_2 = CH_3, R_1 = *o*-F-C_6H_4 (**13**), *m*-F-C_6H_4 (**14**), *p*-F-C_6H_4 (**15**), C_6H_{11} (**16**), CH_2OH (**17**).

R_2 = CH_3, R_1 = Ph (**18**).

Scheme 1. Synthetic route to the target compounds **6-18**.

The semi-pure furans **3** were then condensed with formamide in a formic acid/DMF mixture at 150 °C. The product **4** could also be precipitated from water giving isolated yields in the range of 38 to 63% from **3**. Compounds **4** were then chlorinated using neat $POCl_3$ leading to the formation of the 6-aryl-furopyrimidines **5**. Isolated yields were for most compounds in the range of 75 - 89%. However, a low 16% yield was seen for the more labile cyano derivative. A decrease in yield was also noticed when reactions were performed with stored materials of **4**, indicating lability issues also with the furopyrimidones. Compounds **5a-g** were all treated with (*R*)-1-phenylethylamine to furnish the corresponding end-products **6a-g**. Additionally, derivative **5a** was converted to **7a-18a** using various primary amines. The reactions were in most cases performed using *n*-butanol as solvent at reflux giving the products in 73 - 89% yield.

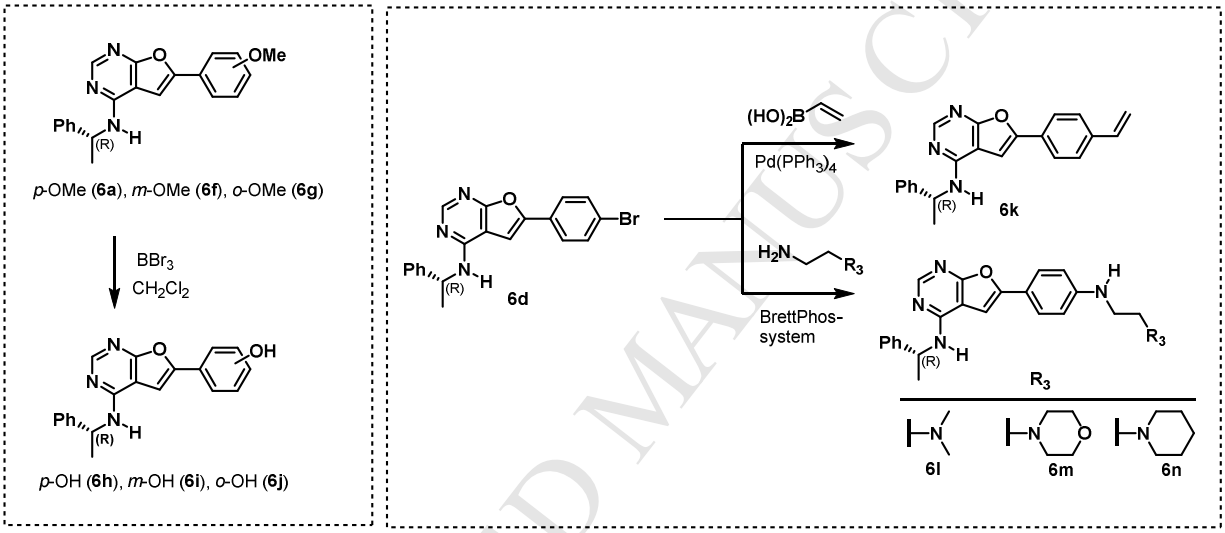

Scheme 2. Post modifications on derivatives **6a**, **6d**, **6f** and **6g**.

The subsequent deprotection of the methyl ethers **6a**, **6f** and **6g** using BBr_3 gave the phenolic analogues **6h, 6i** and **6j** in 76 - 82% isolated yield (Scheme 2). The bromo derivative **6d** was applied in both Suzuki and Buchwald type coupling to yield the vinyl analogue **6k** and the amine containing derivatives **6l-n**, see Scheme 2. The purity of all end-products was analysed by HPLC to be > 96% by area.

2.3 *In vitro* EGFR potency

2.3.1 Effect of modification of the 6-aryl group

The effect of the 6-aryl substitution pattern on the activity was investigated using (*R*)-1-phenylethylamine as the 4-amino group. The choice of the amino group was based on our previous SAR studies on the structurally related thieno- and pyrrolopyrimidines [10, 13]. The activities in terms of IC_{50} values are summarised in Figure 3.

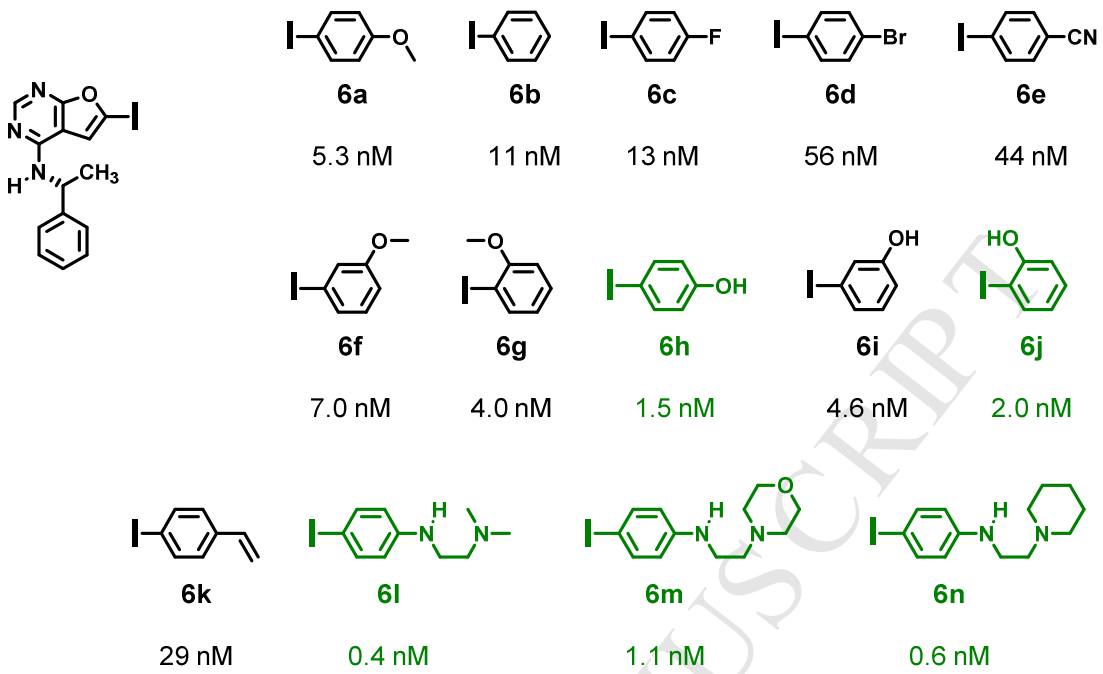

Figure 3. Effect of variation of the 6-aryl group on the EGFR IC_{50} value (nM). (The supplementary material file contain information on number of measurements and standard deviations).

We initially evaluated the derivatives **6a-k** in EGFR assays. The highest activity was seen for compounds having electron donating substituents in *ortho* and *para* position, of which the most potent derivatives were the phenols **6h** and **6j**. The binding interactions between EGFR and derivatives **6b**, **6g, 6h** (see Supplementary Material) and **6j** (see Figure 4) were investigated by induced-fit docking with Schrödinger [26-28], and 10 ns molecular dynamics using the Desmond suite, the OPL-3 force field and the TIP4P solvent model [29]. The common binding motif seen for the four analogues includes a hydrogen bond between N-1 and Met793, a water mediated interaction between N-3 and Thr854, and what appears to be a cation-π interaction between the aromatic part of the 4-amino group and Lys745. The *ortho*-phenolic compound **6j** is indicated to bind via two bridging water molecules to Cys797 and Leu719, which may explain the high potency of this derivative. Dynamics also revealed compound **6b** to interact with Tyr998 via an unconventional hydrogen bond from the *para*-position of the ligand to the Tyr998 centroid. This H-bond was not judged important for compound **6g** and **6j**. The unsubstituted derivative **6b**, and compounds with more lipophilic substituents at the *para* position such as fluorine (**6c**), bromine (**6d**) or vinyl (**6k**) displayed lower inhibitory potency. A mediocre activity was also noticed for the *para*-cyano containing compound **6e**.

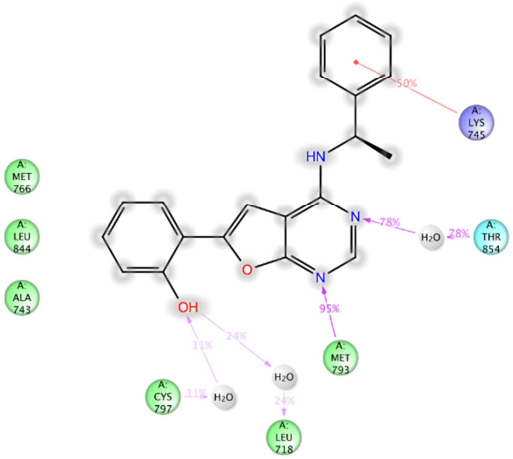

Figure 4. EGFR ligand interactions as identified by docking and molecular dynamics for **6j**. (The 2D representation of the 3-dimentional image wrongly shows the position of the *ortho* substituent.) Docking and dynamics showed these to have an anti-relationship to the furan oxygen.

Solubilising tails placed in *para* position of the 6-aryl group boosted potency for our related thienopyrimidines [9]. As the initial structure-activity relationship data for the furopyrimidines corresponded fairly well with that observed for the thieno-series, we expected that structurally related furopyrimidines should be active. Molecular docking of **6l**-**6n** resulted in superior docking scores, which strengthened our assumption. Indeed, this turned out to be the case, and the most potent derivative **6l**, bearing a *N'*,*N'*-dimethylethane-1,2-diamine group had an IC_{50} value of 0.4 nM, which is equipotent with the commercial drug Erlotinib. The piperidine containing compound **6n** was slightly less potent (IC_{50}: 0.6 nM), while the morpholine analogue had an IC_{50} of 1.1 nM. The IC_{50} titration curves of compounds **6b**, **6j**, **6l** and **6n** are compared in Figure 5.

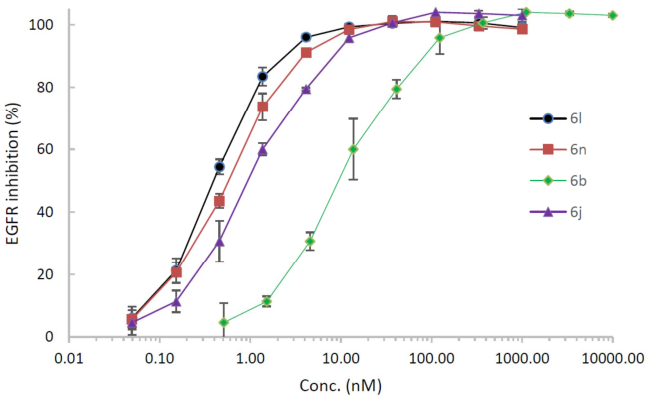

Figure 5. IC_{50} curves with error bars of **6b** (20 data points), **6j** (20 data points), **6l** (40 data points) and **6n** (40 data points).

Binding interactions for **6l** (Figure 6) and **6n** (Supplementary Material) as analysed by docking followed by 10 ns dynamics, revealed the pyrimidine core and Fragment A to be positioned similar to that seen for **6b**, **6g**, **6h** and **6j**. Further, the higher activity of these derivatives are indicated to be due to a hydrogen bonding network involving the *N'*,*N'*-dimethylethane-1,2-diamine.

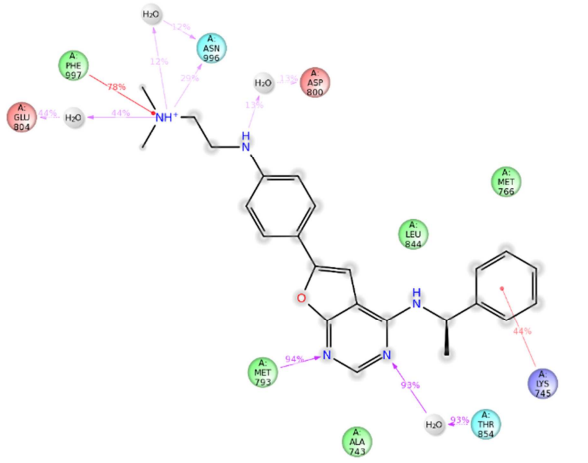

Figure 6. EGFR ligand interactions as identified by docking and molecular dynamics for **6l** (docking score: -12.47).

2.3.2 Effect of variation of the 4-amino group

Then the effect of varying the amine part (Fragment A) was investigated with 14 different amines, using *para*-methoxyphenyl as the 6-aryl group (**a**-series), see Figure 7.

When installing alcohol groups in the R_2-substituent (compound (*S*)-**7a** and (*R*)-**12a**), the potency increased slightly compared with the benchmark (*R*)-configurated **6a**. Note that the change in absolute configuration is due to the Cahn-Ingold-Prelog priority rules, and not a switch in stereopreference. The amide containing racemate **11a** also demonstrated decent activity. Lower potency was observed for the achiral derivative **8a** and furopyrimidines bearing fluorine substituents at the aromatic ring of Fragment A. To shed light on the involvement of the aromatic ring in EGFR-ligand binding, compound **16a**, in which the phenyl was replaced by a cyclohexyl, and **17a**, lacking the ring system, were prepared and assayed. Both compounds possessed low inhibitory potency, revealing the crucial role of the aromatic ring in binding with EGFR. This conclusion is in line with the interaction maps shown in Figure 4 and 6 and what was observed in a study of thienopyrimidine based EGFR inhibitors [30]. The (*S*)-configurated derivative **18a** also had a low activity, which corresponds with previous findings in the thienopyrimidine series [10, 21]. Clearly, stereochemistry is of uttermost importance for EGFR inhibitory properties.

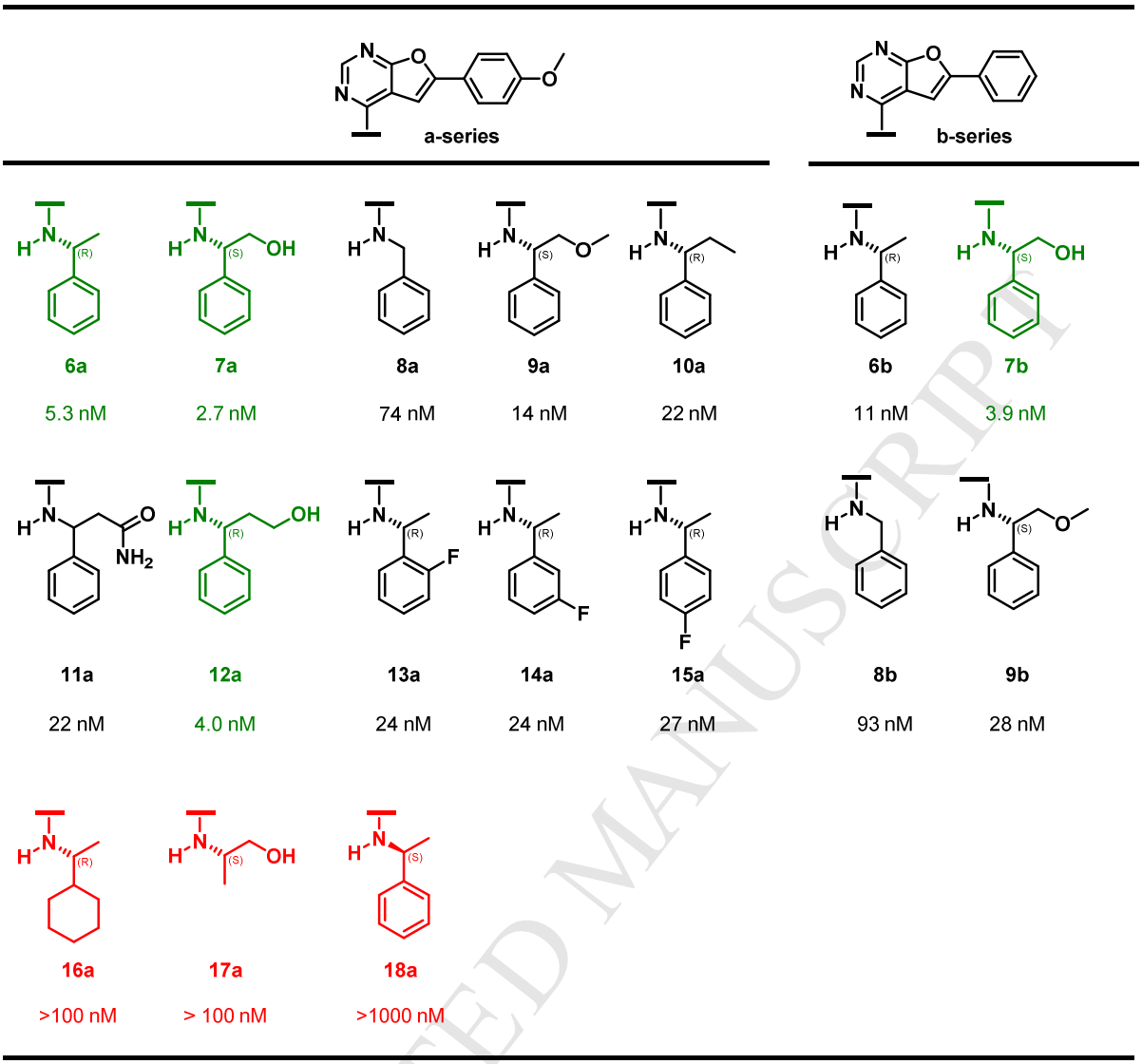

Figure 7. Effect of varying the 4-amino group in the a-series on the EGFR IC_{50} values. (The Supplementary Material file contain information on number of measurements and standard deviations).

The major trend with respect to the effect of the 4-amino group on potency was similar also in the **b**-series of compounds (4 examples, see Figure 7), which indicate very similar binding mode. This further motivated us for combination of activity inducing groups into the same molecule. Thus, we merged the functionality in compound **6h** and **7b** into the derivative **7h**, see Figure 8.

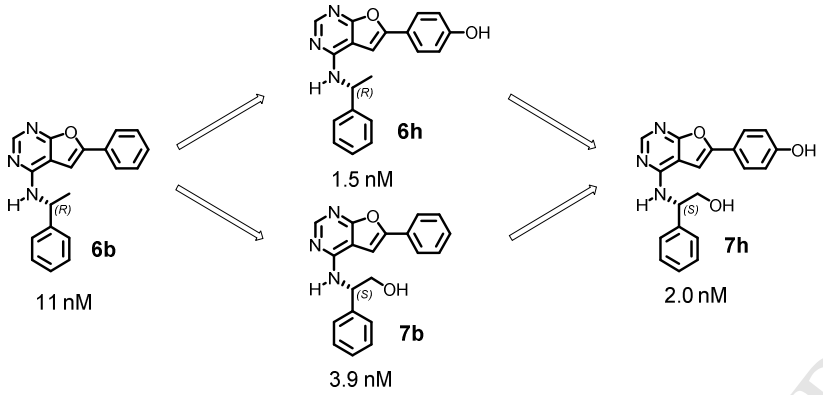

Figure 8. Attempts to improve potency by combining activity inducing fragments.

Whereas compound **7h** was fairly potent (IC_{50} of 2.0 nM), no improvement in activity was seen as compared to derivative **6h**. A possible reason could be that the desolvation cost for this rather polar molecule is high as compared to the gain in protein-ligand binding energy.

2.3.3 Structure-activity relationship

The structure-activity relationship (SAR) information obtained, summarised in Figure 9, shows that the major activity cliffs are when changing the amine part of Fragment A to aliphatic amines or to amines having the opposite stereochemistry. Highest EGFR activity was seen when R_2 was hydroxymethyl, hydroxyethyl or methyl.

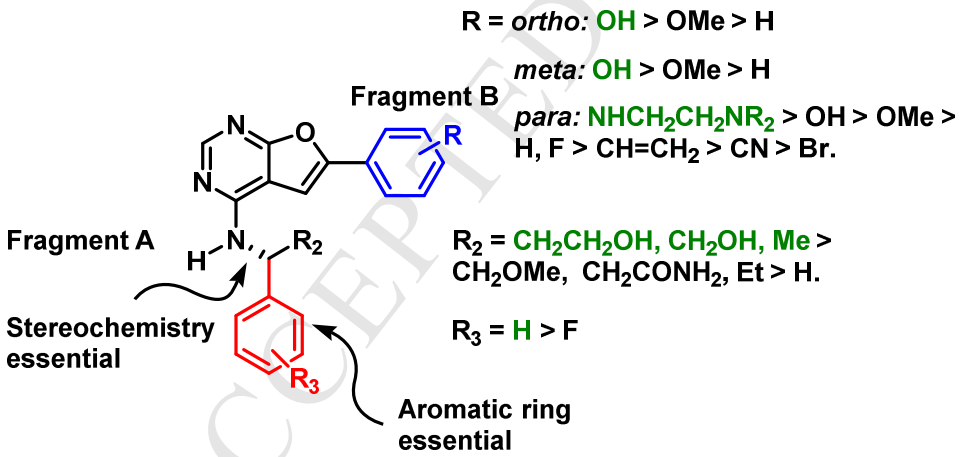

Figure 9. Structure activity relationship data obtained in this study.

Substitution of the 6-aryl group (Fragment B) allows for fine tuning of potency. Polar substituents are preferred in terms of activity, and a boost in potency was seen for compounds containing the $NHCH_2CH_2NMe_2$ substituent in *para* position. Our previous studies on thienopyrimidines [9, 10] did not contain data on compounds containing aliphatic amines in Fragment A, or compounds containing $NHCH_2CH_2NR_2$ groups in *para* position of Fragment B. However, Figure 10 compares the IC_{50} values for those furopyrimidines in which the corresponding thieno- or pyrrolopyrimidines also have been assayed for EGFR activity.

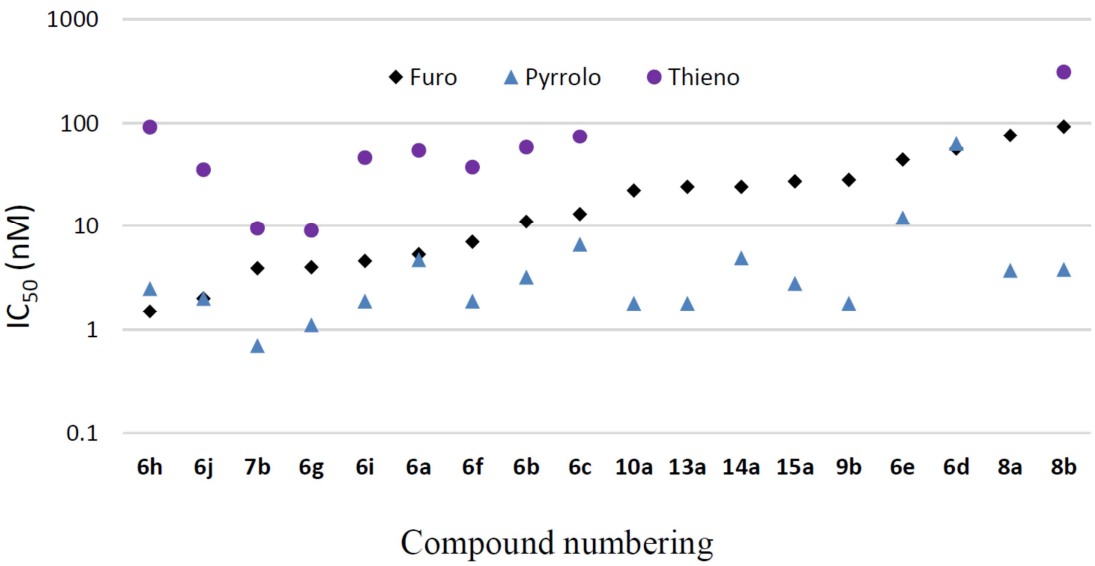

Figure 10. Effect of scaffold hopping: EGFR activity of furo- vs. thieno- and pyrrolopyrimidines. Numbering corresponds to the structure of the furopyrimidines. The comparison contains data for 18 furopyrimidines, 18 pyrrolopyrimidines [13, 22] and 10 thienopyrimidines [9, 10].

The comparison reveals that the furopyrimidines on average results in more potent EGFR inhibitors than the corresponding thienopyrimidines. The largest difference in activity between the two scaffolds was for the *para*- and *ortho*-phenolic compounds **6h** and **6j** and their thienopyrimidine counterparts. Molecular docking and dynamics were employed to aid understanding of these differences. An overlay of the docked conformers of **6j** and the corresponding thienopyrimidine is shown in Figure 11.

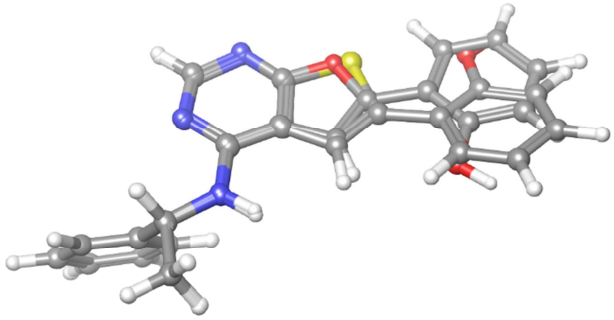

Figure 11. Overlay of the docked structures **6j** and the corresponding thienopyrimidine analogue.

As seen, the longer C-S bond lengths of the thienopyrimidines as opposed to the C-O bond in furopyrimidines leads to a slight difference in the position of the 6-aryl group for the two scaffolds. Thus, dynamics finds that the *para*-phenolic group engage in hydrogen bonding with water molecules coordinated to different amino acid residues (see Supplementary Material). Secondly, compound **6j** appears to have the phenolic group in an *anti*, rather than *syn* relationship relative to the furan oxygen. The thienopyrimidine analogue on the other hand prefers a *syn* relationship, which might be explained by weak intramolecular O-S interactions [31, 32]. Thus, computational chemistry predicts that the *ortho*-phenolic group of **6j** interacts *via* two water molecules to Cys797 and Leu718 as shown in Figure 4. The *ortho*-phenolic group in the thienopyrimidine analogue seems to be bonded via a water molecule to Pro797 (Supplementary Material). The superior activity of the pyrrolopyrimidines is explained by additional hydrogen bonding involving the pyrrolo N-H function. Overall, the furopyrimidines appears as an attractive alternative to both quinazolines and thienopyrimidines in development of EGFR inhibitors.

2.3.4 Kinase profiling and cell model

The two most potent furopyrimidines identified **6l** and **6n**, were profiled towards a panel of 50 additional kinases at 500 nM test concentration and compared with the profile of Erlotinib. Gini plots and Gini coefficients [33] (see Supplementary Materials) revealed a similar average selectivity profile. However, the fingerprint pattern was somewhat different. Figure 12 shows the main off-targets sorted by the activity displayed by compound **6n**.

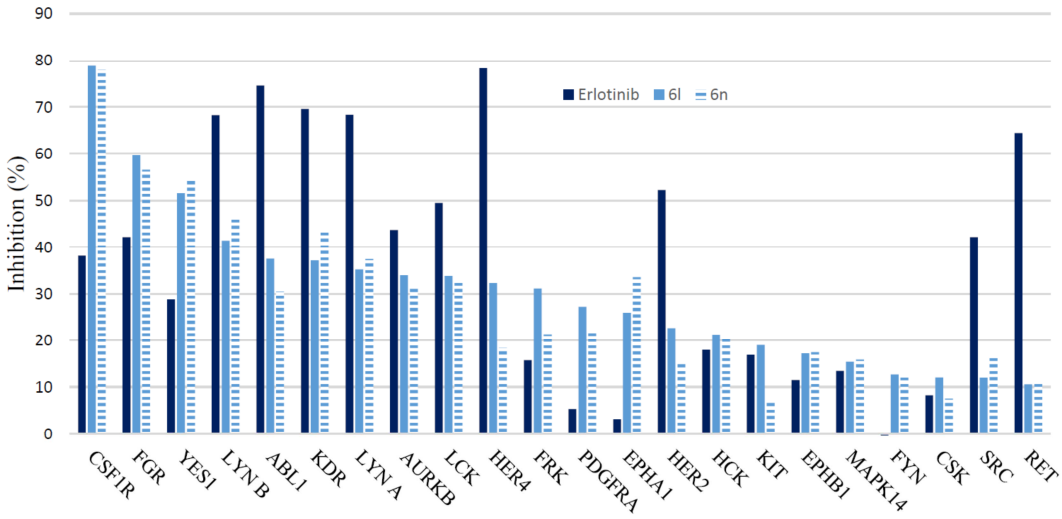

Figure 12. Kinase inhibition profile of **6l**, **6n** and Erlotinib sorted by the activity of **6n.**

The main off-targets for the furopyrimidines includes CSF1R, FGR, YES, LYN B and ABL, while low activity was seen towards HER2 and HER4. Inhibitors having dual activity towards EGFR and CSF1R might be of value in treatment of glioblastoma [34]. Erlotinib in

this panel had a higher inhibition than the furopyrimidines towards especially HER2 and HER4, LYN A and B, KDR, Src and RET.

To reveal if the new furopyrimidines **6l** and **6n** also had on-target cellular potency, they were compared with Erlotinib using Ba/F3-EGFR^{L858R} reporter cells [35]. This system consists of a murine bone marrow–derived cell line, which is dependent on interleukin-3 (IL-3), but is rendered IL-3 independent by stable expression of the EGFR^{L858R} oncogene. Cell proliferation studies using the XTT assay proved both compounds to be active in the nanomolar concentration range, with IC_{50} of 217 and 196 nM for **6l** and **6n**, respectively. Erlotinib in this assay had an IC_{50} of 87 nM, see Figure 13.

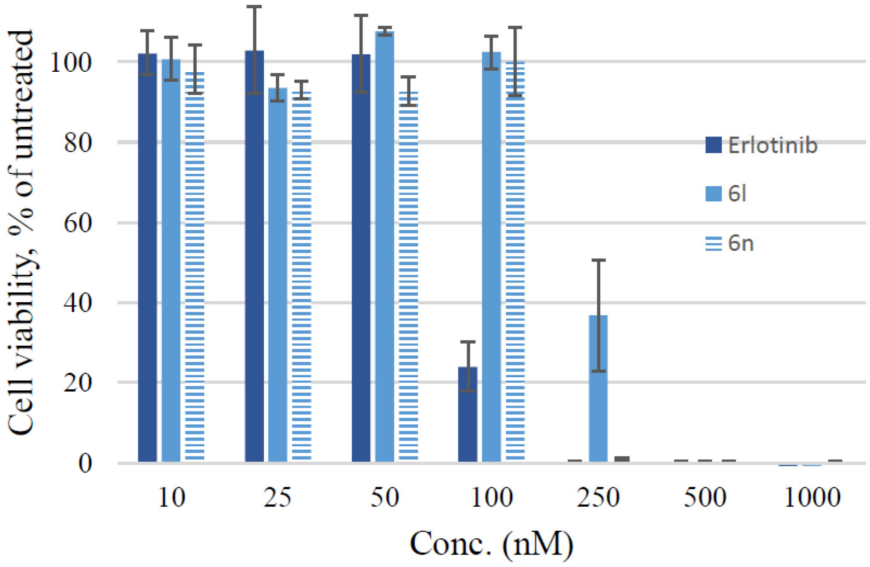

Figure 13. Cell proliferation study of compounds **6l** and **6n** compared to Erlotinib using Ba/F3-EGFR^{L858R} cells. Each data point shown is the average of three independent replicates. IC_{50}: Erlotinib: 87±5; **6l**: 217±24, **6n**: 196±6.

3 Conclusion

Based on the furopyrimidine scaffold, a structure-activity investigation on EGFR has been performed. The study showed that the activity was highly dependent on the substitution pattern. In the 4-amino group, both the presence of a stereocentre with correct stereochemistry and an unsubstituted phenyl ring boosts potency. Experimental and *in silico* data indicate this to be partly due to favourable cation-π interactions. Preferable substituents in the 6-aryl group includes solubilising tails containing amine functionality. The most potent derivative was equipotent to the commercial drug Erlotinib, and profiling in a panel of 50 kinases revealed this compound to have other kinase off-targets, most importantly CSF1R. Additionally, cellular studies using engineered Ba/F3 EGFR^{L858R} cells showed two of the furopyrimidines to have IC_{50} values in the nanomolar range. By comparing the EGFR activity of furopyrimidines with that of the corresponding thieno- and pyrrolopyrimidines, the

furopyrimidine was concluded to be an attractive scaffold for further development. Thus, new active EGFR based inhibitors are likely to be found by further exploring the substitution pattern of the *meta*- and *para* position of the 6-aryl group using polar substituents.

Experimental

4.1 General

1st generation BrettPhos, BrettPhos, $NaBH_4$, boronic esters/acids, all the α-acetophenones and nearly all amines were from Sigma Aldrich. (*S*)-2-Methoxy-1-phenylethanamine was prepared and characterized in other studies from our laboratory [10]. (*R*)-3-Amino-3-phenylpropan-1-ol was from Fluorochem. Silica-gel column chromatography was performed using silica-gel 60A from Fluka, pore size 40-63 µm. Celite 545 from Fluka was also used.

4.2 Analyses

^1H and ^{13}C NMR spectra were recorded with Bruker Avance 400 spectrometer operating at 400 MHz and 100 MHz, respectively. ^{19}F NMR was performed on a Bruker Avance 500 operating at 564 MHz. For ^1H and ^{13}C NMR chemical shifts are in ppm rel. to DMSO-d_6, while for ^{19}F NMR the shift values are relative to hexafluorobenzene. Coupling constants are in hertz. HPLC (Agilent 110-Series) with a G1379A degasser, G1311A Quatpump, G1313A ALS autosampler and a G1315D Agilent detector (230 nm) was used to determine the purity of the synthesised compounds. All compounds evaluated for EGFR inhibitory potency had a purity of ≥96%. Conditions: Poroshell C18 (100×4.6 mm) column, flow rate 0.8 mL/min, elution starting with water/CH_3CN (90/10), 5 min isocratic elution, then linear gradient elution for 35 min ending at CH_3CN/water (100/0). The software used with the HPLC was Agilent ChemStation. Accurate mass determination (ESI) was performed on an Agilent G1969 TOF MS instrument equipped with a dual electrospray ion source. Accurate mass determination in positive and negative mode was performed on a "Synapt G2-S" Q-TOF instrument from Waters. Samples were ionized by the use of an ASAP probe, no chromatography separation was used before the mass analysis. FTIR spectra were recorded on a Thermo Nicolet Avatar 330 infrared spectrophotometer. All melting points are uncorrected and measured by a Stuart automatic melting point SMP40 apparatus.

4.3 *In vitro* EGFR (ErbB1) inhibitory potency

The compounds were supplied in a 10 mM DMSO solution, and enzymatic EGFR (ErbB1) inhibition potency was determined by Thermo Fisher Scientific (LifeTechnology) using their Z'-LYTE® assay technology[36]. All compounds were first tested for their inhibitory activity at 100 nM in duplicates. The potency observed at 100 nM was used to set starting point of the IC_{50} titration curve, in which three levels were used 100, 1000 or 10000 nM. The IC_{50} values reported are based on the average of at least 2 titration curves (minimum 20 data points), and were calculated from activity data with a four parameter logistic model using SigmaPlot (Windows Version 12.0 from Systat Software, Inc.) Unless stated otherwise the ATP concentration used was equal to K_m. The average standard deviation for single point measurements were <4%.

4.4 *In vitro* kinase panel

The compounds were supplied in a 10 mM DMSO solution, and enzymatic kinase inhibition potency was determined by Thermo Fisher Scientific (LifeTechnology) using their Z'-LYTE® assay technology [1], at 500 nM in duplicates. ATP concentration used was equal to K_m, except when this service was not provided and other concentrations had to be used.

4.5 Ba/F3 reporter cell analysis

Transfected Ba/F3 cells containing expression vectors for the $EGFR^{L858R}$ mutant was a kind gift from Dr. Nikolas von Bubnoff at the Technical University of Munich, Munich, Germany [35]. The cells were cultured in RPMI 1640 (Gibco, Invitrogen) supplemented with 10% FCS (Gibco, Invitrogen), 1% L-glutamine (Gibco, Invitrogen) and 0.1% Gentamycin (Sanofi Aventis). Erlotinib was purchased from LC Laboratories (Woburn, MA). All inhibitors were reconstituted in DMSO, and appropriate stock solutions were prepared using cell culture medium. The final percentage concentrations of DMSO were < 0.2%. Proliferation analysis: Ba/F3 cells (1×10^4 per well) were plated into 96-well plates. Inhibitors were added in different concentrations as indicated. Cell growth was measured at 48 hours using TACS® XTT Cell Proliferation Assay (Trevigen) according to the manufacturer's instructions. Three independent biological experiments were performed for each compound. All measurements were performed in triplicate.

4.6.1 3-Amino-3-phenylpropanoic acid [37].

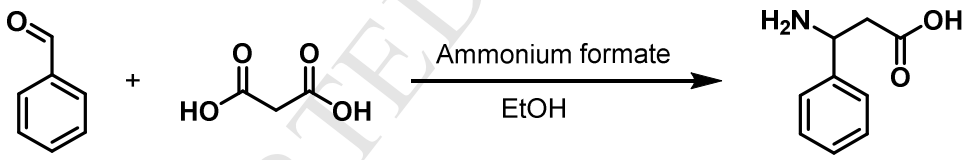

Malonic acid (9.81 g, 94.0 mmol) and ammonium formate (11.9 g, 188 mmol) were slurried in EtOH (33 mL, 96%) at ambient temperature and heated to 60 °C. Benzaldehyde (9.5 mL, 943.5 mmol) was added and temperature maintained below 65 °C. The reaction was reflux for 4 h and cooled to ambient temperature overnight. The reaction mixture was filtered, the product washed with EtOH (10 mL) and dried *in vacuo* to yield 7.55 g of 3-amino-3-phenylpropanoic acid as a white solid (45.1 mmol, 48%); mp: 223 - 224 °C (lit. 216 - 218 °C [38], 224 °C [37]); ^{1}H NMR (400 MHz, D_2O): 7.52 - 7.45 (m, 5H), 4.67 (t, J = 6.9, 1H), 2.96 - 2.81 (m, 2H). ^{1}H NMR spectroscopy match that previously reported [37].

4.6.2 Methyl 3-amino-3-phenylpropanoate [37].

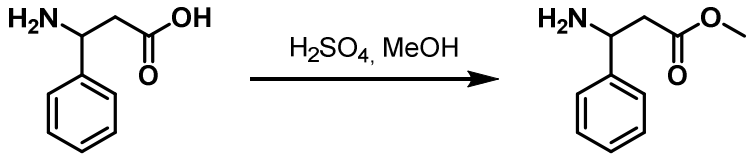

3-Amino-3-phenylpropanoic acid (2.00 g, 12.1 mmol) was slurried in MeOH (13 mL) and cooled to -10 ^{o}C. Concentrated H_2SO_4 (1.3 mL) was added over 45 min, maintaining the temperature below 0 ^{o}C. Once completion of the addition, the reaction was heated up to ambient temperature and stirred for 5 h. The reaction mixture was reduced by half *in vacuo* followed by addition of CH_2Cl_2 (2 x 14 mL). The pH of aqueous layer was adjusted with NaOH (58 mL, 1M) to pH 12. The phases were separated and the organic phases were washed with H_2O (10 mL), dried over anhydrous Na_2SO_4 and concentrated in *in vacuo* to obtain 2.02 g (11.1 mmol, 92%) of methyl 3-amino-3-phenylpropanoate as an clear oil; ^{1}H NMR (400 MHz, $CDCl_3$-TMS): 7.36 - 7.24 (m, 5H), 4.42 (t, *J* = 6.9, 1H), 3.68 (s, 3H), 2.67 - 2.65 (m, 2H), 1.74 (s, br, 2H). ^{1}H NMR spectroscopy match that previously reported [37].

4.6.3 3-Amino-3-propanamide [39].

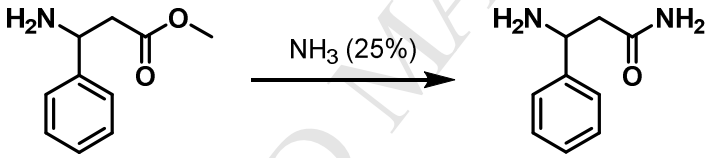

Methyl 3-amino-3-phenylpropanoate (2.00 g, 11.2 mmol) was slurried in ammonia (25 mL, 25%) and stirred at ambient temperature overnight. The clear reaction mixture was neutralised with aqueous NH_4Cl (40 mL) and extracted with CH_2Cl_2 (2 x 40 mL). The combined organic phases were dried over anhydrous Na_2SO_4 and concentrated *in vacuo* to obtain 1.38 g (8.48, 76%) of 3-amino-3-propanamide as a white crystalline solid; mp 102 - 104 ^{o}C (lit. 99 – 101 ^{o}C [39], 110 ^{o}C [40]) ^{1}H NMR (400 MHz, $CDCl_3$-TMS): 7.38 - 7.25 (m, 5H), 6.89 (s, br, 1H), 5.60 (s, br, 1H), 4.35 (t, *J* = 6.9, 1H), 2.56 - 2.54 (m, 2H), 1.75 (s, br, 2H). ^{1}H NMR spectroscopy match that previously reported [39, 40]

4.6.4 Synthesis of 2-(2-(4-methoxyphenyl)-2-oxoethyl)malononitrile (2a) [41].

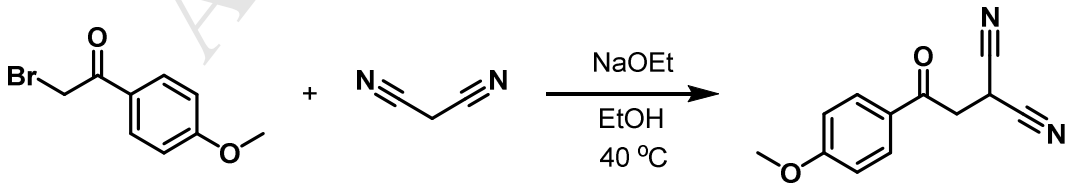

2-Bromo-1-(4-methoxyphenyl)ethan-1-one (**1a**) (2.00 g, 8.73 mmol) was dissolved in ethanol (50 mL) with malononitrile (606 mg, 9.17 mmol) and sodium ethoxide (653 mg, 9.60 mmol). The reaction mixture was heated at 40 °C for 18 h before the solvent was removed under reduced pressure. The crude product was triturated in cold methanol, filtrated and dried *in*

vacuo. This yielded 1.25 g (5.85 mmol, 67%) of **2a** as a white solid; mp: 148 - 154 °C; HPLC purity: 99%, t_R = 18.6 min; ^{1}H NMR (400 MHz, $CDCl_3$-TMS): δ: 7.93 (d, *J* = 8.9, 2H), 6.99 (d, *J* = 9.0, 2H), 4.41 (t, *J* = 6.9, 1H), 3.90 (s, 3H), 3.71 (d, *J* = 6.7, 3H); ^{13}C NMR (100 MHz, DMSO-d_6): δ: 193.0, 164.4, 131.1, 128.3 (2C), 115.0 (2C), 114.6 (2C), 56.1, 38.3, 18.5; IR (neat, cm^{-1}): 2907, 1673, 1602, 1574, 1256, 1178, 1018, 834, 810, 574; HRMS (APCI/ASAP, m/z): 215.0822 (calcd. $C_{12}H_{11}N_2O_2$, 215.0821, $[M+H]^+$). ^{1}H NMR spectroscopy match that previously reported[42].

4.7 General procedure synthesis of 2-amino-5-arylfurane-3-carboxynitriles (3)

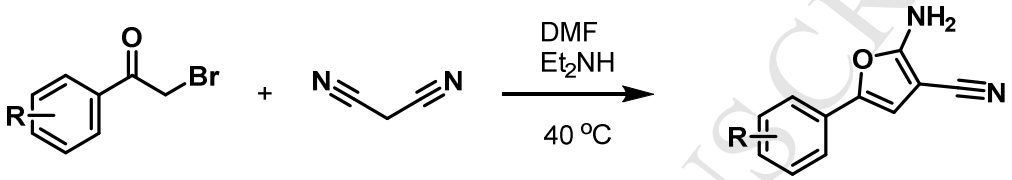

R = 4-OMe **(3a),** H **(3b),** 4-F **(3c),** 4-Br **(3d),** 4-CN **(3e),** 3-OMe **(3f),** 2-OMe **(3g)**

A solution of bromoketone (6 - 25 g) and malononitrile (1.3 eq.) was stirred at 0 °C in DMF (6 mL/g) for 10 min. Diethylamine (2.2 eq) was added at 0 °C over 30 min using a syringe pump and the mixture was stirred at 22 °C for 4.5 h. The solution was poured onto water and left standing for 24 h at 0 ˚C. The formed precipitate was filtered off, washed with water (2 × 50 mL) and petroleum ether (50 mL) and dried *in vacuo* to yield target compound.

4.7.1 2-Amino-5-(4-methoxyphenyl)furan-3-carbonitrile (3a) [42].

Compound **3a** was prepared as described in Section 4.7 starting with 2-bromo-1-(4-methoxyphenyl)ethan-1-one (20.0 g, 87.3 mmol) and malononitrile (7.50 g, 114 mmol). This gave 7.00 g (32.7 mmol, 37%) as a brown solid, mp 178 °C (dec.); ^{1}H NMR (400 MHz, DMSO-d_6) δ: 7.49 (s, 2 H), 7.42 (d, *J* = 8.8, 2 H), 6.95 (d, *J* = 8.8, 2H), 6.79 (s, 1 H), 3.76 (s, 3 H); ^{13}C NMR (100 MHz, DMSO-d_6) δ: 164.2, 158.6, 142.5, 124.2 (2C), 122.8, 116.7, 114.8 (2C), 104.9, 66.3, 55.6; IR (neat, cm^{-1}): 3413, 3327, 2205, 1646, 1508, 1245, 1026, 828; HRMS (EI): 214.0733 (calcd $C_{12}H_{10}N_2O_2$, 214.0737, $[M]^+$). The previous ^{1}H NMR reported in DMSO-d_6 differs with respect to the shift of the NH_2 protons[42].

4.7.2 2-Amino-5-phenylfuran-3-carbonitrile (3b) [43].

Compound **3b** was prepared as described in Section 4.7 starting with 2-bromo-1-phenylethan-1-one (19.0 g, 95.6 mmol) and malononitrile (8.21 g, 124 mmol). This gave 8.61 g (46.7 mmol, 49%) of **3b** as a brown solid; mp 193 °C (dec.) (lit. [44] 196-198°C); ^{1}H NMR (400 MHz, DMSO-d_6) δ: 7.61 (s, 2 H), 7.49 - 7.47 (m, 2 H),7.38 - 7.34 (m, 2H), 7.21 - 7.18 (m, 1 H), 6.98 (s, 1 H); ^{13}C NMR (100 MHz, DMSO-d_6) δ: 164.0, 141.8, 129.4, 128.8 (2C), 126.6, 122.1 (2C), 116.1, 106.7, 66.2; IR (neat, cm^{-1}): 3412, 3323, 3112, 2206, 1645, 1610 1173, 754; HRMS (ESI): 185.0712 (calcd $C_{11}H_9N_2O$, 185.0715, $(M+H)^+$).

4.7.3 2-Amino-5-(4-fluorophenyl)furan-3-carbonitrile (3c)

Compound **3c** was prepared as described in Section 4.7 starting with 2-bromo-1-(4-fluorophenyl)ethan-1-one (21.5 g, 97.0 mmol) and malononitrile (8.33 g, 126 mmol). This gave 12.4 g (61.2 mmol, 63%) of **3c** as a brown solid. mp 156 °C (dec.); ^{1}H NMR (400 MHz, DMSO-d_6) δ: 7.60 (s, 2H), 7.52 - 7.49 (m, 2H), 7.23 - 7.19 (m, 2H), 6.95 (s, 1H); ^{13}C NMR (100 MHz, DMSO-d_6) δ: 164.0, 162.3, 160.8 (d, J = 244.2), 141.1, 126.1 (d, J = 3.1), 124.1 (d, J = 8.1, 2C), 116.0, 115.9 (d, J = 22.0, 2C), 106.5; IR (neat, cm^{-1}): 3408, 3322, 3252, 3197, 2205, 1643, 1571, 1500, 1232, 836; HRMS (APCI/ASAP, m/z): 203.0621 (calcd. $C_{11}H_8FN_2O$, 203.0621, $[M+H]^+$).

4.7.4 2-Amino-5-(4-bromophenyl)furan-3-carbonitrile (3d) [45].

Compound **3d** was prepared as described in Section 4.7 starting with 2-bromo-1-(4-bromophenyl)ethan-1-one (15.0 g, 54.0 mmol) and malononitrile (4.64 g, 70.2 mmol). This gave **3d** in 6.55 g (24.9 mmol, 48%) as a brown solid; mp 182 °C (dec.); ^{1}H NMR (400 MHz, DMSO-d_6) δ: 7.69 (s, 2H), 7.56 (d, J = 8.6, 2H), 7.42 (d, J = 8.6, 2H), 7.08 (s, 1H); 13C NMR (100 MHz, DMSO-d_6) δ: 164.6, 141.2, 132.2 (2C), 129.0, 124.4 (2C), 119.8, 116.4, 108.4, 66.9; IR (neat, cm^{-1}): 3411, 3311, 2219, 1646, 1578, 824, 803; HRMS (EI): 261.9737 (calc for $C_{11}H_7ON_2Br$, 261.9736, $[M]^+$).

4.7.5 2-Amino-5-(4-cyanophenyl)furan-3-carbonitrile (3e) [42].

Compound **3d** was prepared as described in Section 4.7 starting with 2-bromo-1-(4-cyanophenyl)ethan-1-one (6.00 g, 26.8 mmol) and malononitrile (1.91 g, 28.9 mmol) using a reaction time of 17 hours. This yielded 4.51 g (21.6 mmol, 75 %) of a yellow solid; mp. 245 - 254 °C (lit. 240 - 241 °C); ^{1}H NMR (400 MHz, DMSO-d_6) δ: 7.90 (s, 2H), 7.80 (app. d, J = 7.8, 2H), 7.60 (app. d, J = 8.4, 2H), 7.33 (s, 1H); ^{13}C NMR (100 MHz, DMSO-d_6) δ: 165.1, 140.4, 133.7, 133.3 (2C), 122.6 (2C), 119.5, 116.0, 111.9, 108.3, 67.8; IR (neat, cm^{-1}): 3441, 3334, 2232, 2211, 1631, 1604, 1577, 1173, 830, 805; HRMS (EI): 210.0733 (calcd. $C_{12}H_8N_2O_2$, 210.0736, $[M]^+$). The ^{1}NMR shift data corresponds with that previously reported [42].

4.7.6 2-Amino-5-(3-methoxyphenyl)furan-3-carbonitrile (3f)

Compound **3f** was prepared as described in Section 4.7 starting with 2-bromo-1-(3-methoxyphenyl)ethan-1-one (25.0 g, 109 mmol) and malononitrile (9.37 g, 142 mmol). This resulted in 13.7 g (64.0 mmol, 59%) as a brown solid, mp 180 °C (dec.); ^{1}H NMR (400 MHz, DMSO-d_6) δ: 7.61 (s, 2H), 7.29 - 7.25 (m, 1H), 7.08 - 7.06 (m, 1H), 7.03 - 7.01 (m, 2H), 6.79 - 6.77 (m, 1H), 3.77 (s, 3H); ^{13}C NMR (100 MHz, DMSO-d$_6$)δ: 164.0, 159.6, 141.6, 130.6, 130.0, 116.1, 114.5, 112.3,107.3, 107.2, 66.2, 55.1; IR (neat, cm^{-1}): 3392, 332, 3210, 2215, 152, 1570,1166, 1047, 768; HRMS (APCI/ASAP, m/z): 215.0817 (calcd. $C_{12}H_{11}N_2O_2$, 215.0821, $[M+H]^+$).

4.7.7 2-Amino-5-(2-methoxyphenyl)furan-3-carbonitrile (3g)

Compound **3g** was prepared as described in Section 4.7 starting with 2-bromo-1-(2-methoxyphenyl)ethan-1-one (10.0 g, 43.7 mmol) and malononitrile (3.75 g, 56.8 mmol). This gave 4.49 g (20.9 mmol, 48%) of **3g** as a brown solid, mp 177 °C (dec.); ^{1}H NMR (400 MHz,

DMSO-d_6) δ: 7.59 (s, 2H), 7.48 - 7.45 (m, 1H), 7.23 - 7.18 (m, 1H), 7.08 - 7.05 (m, 1H), 7.01 - 6.96 (m, 1H), 6.85 (s, 1H), 3.89 (s, 3H); ^{13}C NMR (100 MHz, DMSO-d_6) δ: 163.8, 154.8, 139.0, 128.1, 124.0, 121.1, 118.5, 116.7, 111.8, 111.3, 66.8, 56.1; IR (neat, cm^{-1}): 3402, 3321, 2206, 1649, 1587, 1242, 1025, 748; HRMS (EI): 214.0740 (calcd. for $C_{12}H_{10}O_2N_2$, 214.0737, $[M]^+$).

4.8 General procedure for preparing 6-aryl-furo[2,3-*d*]pyrimidin-4(3*H*)-one (4)

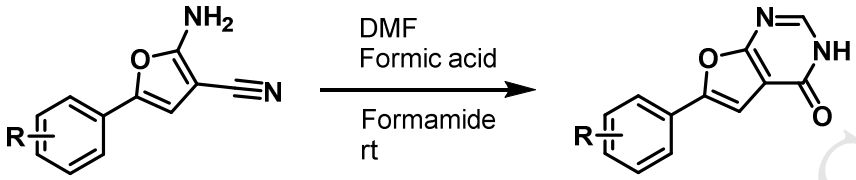

R = 4-OMe **(4a)**, H **(4b)**, 4-F **(4c)**, 4-Br **(4d)**, 4-CN **(4e)**, 3-OMe **(4f)**, 2-OMe **(4g)**

To a solution of **3a - 3g** (0.50 - 13 g), formic acid (23 eq.), anhydrous DMF (30 eq.) and excess of formamide (50 eq.) were added. The mixture was heated at 150 ˚C for 24 h before cooling to 22 ˚C and then isopropanol (50-300 mL) was added. The mixture was left standing for 72 h at 0 ˚C. The formed precipitate was isolated by filtration, washed with cold isopropanol (0.5 - 50 mL) and *n*-hexane (2 × 2 - 15 mL), and drying *in vacuo* giving the target compounds **4a** - **4g**.

4.8.1 6-(4-Methoxyphenyl)furo[2,3-*d*]pyrimidin-4(3*H*)-one (4a)

The reaction was performed as described in Section 4.8 giving 2.01 g (8.31 mmol, 30%) of **4a** as a brown solid; mp > 300 °C; ^{1}H NMR (400 MHz, DMSO-d_6) δ: 12.61 (s, 1H), 8.11 (s, 1H), 7.79 (d, *J* = 8.7, 2H), 7.31 (s, 1H), 7.05 (d, *J* = 8.7, 2H), 3.82 (s, 3H); ^{13}C NMR (100 MHz, DMSO-d_6) δ: 164.6, 160.2, 158.7, 152.1, 146.6, 126.3 (2C), 122.1, 115.0 (2C), 110.0, 99.7, 55.8; IR (neat, cm^{-1}): 3100, 2838, 1674, 1253, 817, 780, 625; HRMS (EI): 242.0691 (calcd $C_{13}H_{10}N_2O_3$, 242.070, $[M]^+$).

4.8.2 Phenylfuro[2,3-*d*]pyrimidin-4(3*H*)-one (4b) [43].

The reaction was performed as described in Section 4.8 starting with **3b** (10.2 g, 55.5 mmol). This gave 4.47 g (21.1 mmol, 38%) of **4b** as a brown solid; mp > 300 °C; ^{1}H NMR (400 MHz, DMSO-d_6) δ: 12.65 (s, 1H), 8.15 (s, 1H), 7.86 - 7.84 (m, 2H), 7.50 - 7.46 (m, 3H), 7.40 - 7.37 (m, 1H); ^{13}C NMR (100 MHz, DMSO-d_6) δ: 164.4, 158.2, 151.2, 146.7, 129.1 (2C), 128.9, 128.7, 124.1 (2C), 109.4, 101.2; IR (neat, cm^{-1}): 3407, 3097, 2851, 1673, 1203, 928, 749; HRMS (APCI/ASAP, m/z): 213.0663 (calcd. $C_{12}H_9N_2O_2$, 213.0664, $[M+H]^+$).

4.8.3 6-(4-Fluorophenyl)furo[2,3-*d*]pyrimidin-4(3*H*)-one (4c)

The reaction was performed as described in Section 4.8 starting with 3c (10.0 g, 49.5 mmol). This gave **4c** in 5.36 g (20.46 mmol, 41%) as a brown solid. mp >300 °C; ^{1}H NMR (400 MHz, DMSO-d_6) δ: 12.65 (s, 1H), 8.14 (s, 1H), 7.92 - 7.87 (m, 2H), 7.46 (s, 1H), 7.36 - 7.30 (m, 2H); ^{13}C NMR (100 MHz, DMSO-d_6) δ: 164.4, 162.2 (d, *J* = 246.6), 158.2, 150.4, 146.7,

126.4 (d, *J* = 8.5, 2C), 125.6 (d, *J* = 3.3), 116.1 (d, *J* = 22.0, 2C), 109.4, 101.1; IR (neat, cm^{-1}): 3411, 3311, 2219, 1646, 1578, 824, 803; HRMS (EI): 261.9737 (calcd. for $C_{12}H_7ON_2F$, 261.9736, $[M]^+$).

4.8.4 6-(4-Bromophenyl)furo[2,3-*d*]pyrimidin-4(3*H*)-one (4d)

The reaction was performed as described in Section 4.8 starting with **3d** (526 mg, 2.00 mmol). This gave 360 mg (1.23 mmol, 61%) of **4d** as brown solid; mp > 300 °C; ^{1}H NMR (400 MHz, DMSO-d_6) δ: 12.68 (s, 1H), 8.17 (s, 1H), 7.81 (d, *J* = 8.6, 2H), 7.68 (d, *J* = 8.6, 2H), 7.56 (s, 1H); ^{13}C NMR (100 MHz, DMSO-d_6) δ: 165.0, 158.7, 150.6, 147.4, 132.5 (2C), 128.7, 126.6 (2C), 122.3, 109.9, 102.6; IR (neat, cm^{-1}): 3413, 3095, 2852, 1676, 928, 815, 779; HRMS (EI): 289.9687 (calcd. for $C_{12}H_7O_2N_2Br$, 289.9685, $[M]^+$)

4.8.5 6-(4-Cyanophenyl)furo[2,3-*d*]pyrimidin-4(3*H*)-one (4e)

The reaction was performed as described in Section 4.8 starting with **3e** (2.00 g, 9.56 mmol). This gave 1.63 g (6.87 mmol, 72%) of a red highly impure solid. NMR spectroscopy was inconclusive on the identity of the components, however HRMS (EI): 238.0613 (calcd. $C_{13}H_{10}N_2O_3$, 238.0617, $[M]^+$) indicated the presence of the target product **4e**.

4.8.6 6-(3-Methoxyphenyl)furo[2,3-*d*]pyrimidin-4(3*H*)-one (4f)

The reaction was performed as described in Section 4.8 starting with **3f** (13.1 g, 61.2 mmol). This gave 4.63 g (21.6 mmol, 35%) of **4f** as a brown solid, mp >300 °C; ^{1}H NMR (400 MHz, DMSO-d_6) δ: 12.64 (s, 1H), 8.14 (s, 1H), 7.52 (s, 1H), 7.44 - 7.37 (m, 3H), 6.97 - 6.94 (m, 1H), 3.83 (s, 3H); ^{13}C NMR (100 MHz, DMSO-d_6) δ: 164.4, 159.7, 158.2, 151.1, 146.7, 130.2 (2C), 116.5, 114.7, 109.4, 109.2, 101.6, 55.3; IR (neat, cm^{-1}): 3392, 3320, 3210, 2215, 1520, 1570, 1166, 1047, 768; HRMS (APCI/ASAP, m/z): 243.0768 (calcd. $C_{13}H_{11}N_2O_3$, 243.0770, $[M+H]^+$).

4.8.7 6-(2-Methoxyphenyl)furo[2,3-*d*]pyrimidin-4(3*H*)-one (4g)

The reaction was performed as described in Section 4.8 starting with **3g** (3.00 g, 14.0 mmol). This gave 1.41 g (5.82 mmol, 42%) of **4g** as a brown solid; mp > 300 °C; ^{1}H NMR (400 MHz, DMSO-d_6)δ: 12.63 (s, 1H), 8.15 (s, 1H), 7.84-7.81 (m, 1H), 7.42 - 7.37 (m, 1H), 7.28 (s, 1H), 7.21 - 7.18 (m, 1H), 7.12-7.08 (m, 1H), 3.98 (s, 3H); ^{13}C NMR (100 MHz, DMSO-d_6)δ: 164.2, 158.7, 156.4, 148.4, 147.1, 130.3, 126.2, 121.3, 117.7, 112.3, 109.8, 105.3, 56.1; IR (neat, cm^{-1}): 3402, 3321, 2206, 1649, 1587, 1242, 1025, 748; HRMS (EI): 242.0688 (calcd $C_{13}H_{10}N_2O_3$, 242.0686, $[M]^+$).

4.9 General procedure synthesis of 6-aryl 4-chloro-furo[2,3-*d*]pyrimidines (5)

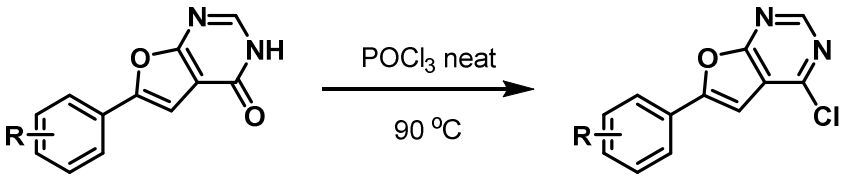

R = H **(5b)**, 4-OMe **(5a)**, 4-F **(5c)**, 4-Br **(5d)**, 4-CN **(5e)**, 3-OMe **(5f)**, 2-OMe **(5g)**

Compounds **4a** - **4g** (0.50 – 4.25 g) and neat $POCl_3$ (0.15 g/mL) were mixed and reacted at 90 ◦C for 3 - 10 h. The solution was poured onto ice and water (5 - 60 mL) was added. NaOH (8 M, 6 - 80 mL) was used to adjust the pH to 12. The precipitated material was isolated by filtration and washed with water (20 - 200 mL) and *n*-pentane (20 - 200 mL). Drying under reduced pressure gave wanted crude products. Purification on silica-gel was performed as described for each individual compound **5a** - **5g**.

4.9.1 4-Chloro-6-(4-methoxyphenyl)furo[2,3-*d*]pyrimidine (5a) [17].

The reaction was performed as described in Section 4.9 starting with compound **4a** (1.71 g, 7.05 mmol). Silica-gel column chromatography (EtOAc, R_f = 0.69) gave 1.65 g (6.34 mmol, 90%) of **5a** as a yellow solid: mp 173 - 174 °C; ^{1}H NMR (400 MHz, DMSO-d_6) δ: 8.78 (s, 1H), 8.01 - 7.98 (m, 2H), 7.59 (s, 1H), 7.15 - 7.12 (m, 2H), 3.86 (s, 3H); ^{13}C NMR (100 MHz, DMSO-d_6) δ: 166.6, 162.6, 156.9, 152.7, 151.2, 127.8 (2C), 120.7, 120.1, 115.3 (2C), 97.0, 55.9; IR (neat, cm^{-1}): 2978, 2842, 1502, 1245, 835, 768; HRMS (EI): 260.0348 (calcd $C_{13}H_9N_2O_2Cl$, 260.0347 $[M]^+$). ^{1}H NMR shifts corresponds with that reported [46].

4.9.2 4-Chloro-6-phenylfuro[2,3-*d*]pyrimidine (5b) [43].

The reaction was performed as described in Section 4.9 starting with compound **4b** (500 mg, 2.36 mmol). Purification by silica-gel column chromatography (EtOAc, R_f = 0.78) gave 412 mg (1.79 mmol, 76%) of **5b** as a yellow solid; mp 152 - 154 °C; ^{1}H NMR (400 MHz, DMSO-d_6) δ: 8.82 (s, 1H), 8.05 - 8.02 (m, 2H), 7.75 (s. 1H), 7.59 - 7.51 (m, 3H); ^{13}C NMR (100 MHz, DMSO-d_6) δ: 166.2, 156.1, 152.7, 151.4, 130.5, 129.3 (2C), 127.8, 125.5 (2C), 119.3, 98.6; IR (neat, cm^{-1}): 3105, 1557, 1252, 756; HRMS (APCI/ASAP, m/z): 231.0329 (calcd. $C_{12}H_8N_2OCl$, 231.0325, $[M+H]^+$).

4.9.3 4-Chloro-6-(4-fluorophenyl)furo[2,3-*d*]pyrimidine (5c)

The reaction was performed as described in Section 4.9 starting with compound **4c** (1.66 g, 7.21 mmol). Purification by silica-gel column chromatography (EtOAC, R_f = 0.73) gave 1.59 g (6.39 mmol, 89%) of **5c** as a yellow solid; mp 172 - 175 °C; ^{1}H NMR (400 MHz, DMSO-d_6) δ: 8.82 (s, 1H), 8.12 - 8.07 (m, 2H), 7.73 (s, 1H), 7.45 - 7.39 (m, 2H); ^{13}C NMR (100 MHz, DMSO-d_6) δ: 166.6, 163.7 (d, J = 249.0), 155.7, 153.2, 151.9, 128.5 (d, J = 8.77, 2C), 124.3 (d, J = 3.4), 119.8, 116.9 (d, J = 22.4, 2C), 99.1; IR (neat, cm^{-1}): 3075, 1502, 1239, 836, 769; HRMS (EI): 248.0150 (calcd. $C_{12}H_6N_2OClF$, 248.0147, $[M]^+$).

4.9.4 6-(4-Bromophenyl)-4-chlorofuro[2,3-*d*]pyrimidine (5d)

The reaction was performed as described in Section 4.9 starting with compound **5d** (4.25 g, 14.5 mmol). Purification by silica-gel column chromatography (*n*-pentane/EtOAc, 1/1, R_f = 0.86) gave 3.99 g (12.9 mmol, 88%) as a yellow solid; mp 193 - 194 °C; ^{1}H NMR (400 MHz, DMSO-d_6) δ: 8.85 (s, 1H), 8.02 - 7.98 (m, 2H), 7.84 (s, 1H), 7.81 - 7.77 (m, 2H); ^{13}C NMR (100 MHz, DMSO-d_6) δ: 166.7, 155.5, 153.5, 152.1, 132.8 (2C), 127.9 (2C), 127.5, 124.4, 119.8, 99.9; IR (neat, cm^{-1}): 3111, 1561, 968, 809, 779; HRMS (EI): 307.9352 (calcd. for $C_{12}H_6ON_2BrCl$, 307.9347, $[M]^+$).

4.9.5 4-(4-Chlorofuro[2,3-*d*]pyrimidin-6-yl)benzonitrile (5e)

Compound **5e** was prepared using the procedure in Section 4.9 using crude material described in Section 3.5.5 (1.50 g). Purification by silica-gel column chromatography (EtOAc, R_f = 0.74) gave 273 mg (1.07 mmol, 17%) of **5e** as a red solid; mp. 170 - 171 °C; HPLC purity: 83%, t_R = 21.9 min; ^{1}H NMR (400 MHz, DMSO-d_6) *δ*: 8.88 (s, 1H), 8.21 (d, *J* = 8.2, 2H), 8.03 (d, *J* = 8.2, 2H), 8.00 (s, 1H); ^{13}C NMR (100 MHz, DMSO-d_6) *δ*: 166.8, 154.5, 154.1, 152.8, 132.7 (2C), 132.4, 126.6 (2C), 119.6, 118.8, 112.9, 102.3; IR (neat, cm^{-1}): 3105, 2922, 2850, 2231, 1563, 1376, 1253, 979, 844, 777; HRMS (APCI/ASAP, m/z): 260.0435 (calcd. $C_{13}H_7ClN_2O$, 260.0431, $[M+H]^+$).

4.9.6 4-Chloro-6-(3-methoxyphenyl)furo[2,3-*d*]pyrimidine (5f) [17].

Compound **5f** was prepared using the procedure in Section 4.9 using compound **4f** (4.00 g, 16.5 mmol). Purification by silica-gel column chromatography (EtOAc, R_f =0.78) gave 3.76 g (14.4 mmol, 87%) of **5f** as a yellow solid; mp 157 - 160 °C; ^{1}H NMR (400 MHz, DMSO-d_6) δ: 8.82 (s, 1H), 7.81 (s, 1H), 7.63 - 7.59 (m, 2H), 7.50 - 7.46 (m, 1H), 7.11 - 7.08 (m, 1H), 3.87 (s, 3H); ^{13}C NMR (100 MHz, DMSO-d_6) δ: 166.2, 159.8, 155.9, 152.8, 151.5, 130.5, 129.1, 119.3, 117.8, 116.8, 110.4, 99.0, 55.5; IR (neat, cm^{-1}): 3103, 1560, 774; HRMS (APCI/ASAP, m/z): 261.0429 (calcd. $C_{13}H_{10}N_2O_2Cl$, 261.0431, $[M+H]^+$).

4.9.7 4-Chloro-6-(2-methoxyphenyl)furo[2,3-*d*]pyrimidine (5g) [17].

Compound **5g** was prepared using the procedure in Section 4.9 using compound **4g** (1.15 g, 4.76 mmol). Purification by silica-gel column chromatography (EtOAc/*n*-pentane 4/1, R_f = 0.60) gave 1.02 g (3.91 mmol, 83%) of **5f** as a yellow solid; mp 156 - 157 °C ; ^{1}H NMR (400 MHz, DMSO-d_6) δ: 8.83 (s, 1H), 8.00 - 7.97 (m, 1H), 7.56 - 7.51 (m, 1H), 7.43 (s, 1H), 7.30 - 7.27 (m, 1H), 7.19-7.15 (m, 1H), 4.04 (s, 3H); ^{13}C NMR (100 MHz, DMSO-d_6) δ: 165.9, 157.6, 153.2 (2C), 152.8, 132.4, 127.6, 121.4, 119.8, 116.4, 112.6, 102.3, 56.4; IR (neat, cm^{-1}): 3075, 1245, 746; HRMS (EI): 260.0349 (calcd. $C_{13}H_9N_2O_2Cl$, 260.0347, [M]+).

4.10 Amination of 6-aryl-4-chlorofuro[2,3-*d*]pyrimidines

Compounds **5a - 5g** (0.125 - 1.84 g) and (*R*)-1-phenylethan-1-amine (3.0 eq.) were added to a dry bottle containing *n*-butanol (1 mL/100 mg) and heated at 145 ˚C for several hours. After cooling down to 22 ˚C, diethyl ether or EtOAc (10 - 150 mL) was added and the mixture was washed with water (15 - 80 mL) and saturated aq. NaCl solution (10 - 60 mL), dried over Na_2SO_4 and concentrated *in vacuo*. Purification on silica-gel as described for the respective compounds **6a - 6g**.

4.10.1 (*R*)-6-(4-Methoxyphenyl)-*N*-(1-phenylethyl)furo[2,3-*d*]pyrimidin-4-amine (6a)

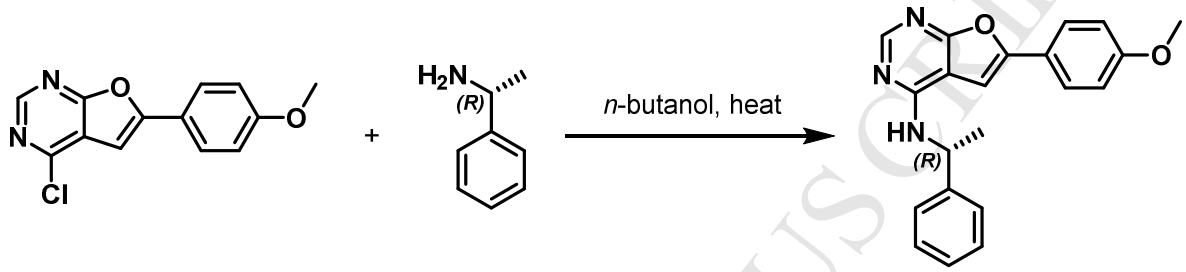

The synthesis was performed as described in Section 4.10 starting with **5a** (350 mg, 1.34 mmol) and (*R*)-1-phenylethan-1-amine (487 mg, 0.52 mL, 4.02 mmol, 3.0 eq.). Silica-gel column chromatography (*n*-pentane/EtOAc 1/1, R_f = 0.63) gave 412 mg (1.19 mmol, 89%) of **6a** as a white solid; mp 131 - 133 ˚C; HPLC purity: 99%, t_R = 30.3 min; $[\alpha]_D^{20}$ = -251.2 (c 1.01, DMSO); ^{1}H NMR (400 MHz, DMSO-d_6): δ: 8.26 - 8.24 (m, 1H), 8.17 (s, 1H), 7.74 - 7.70 (m, 2H), 7.44 - 7.41 (m, 2H), 7.34 - 7.30 (m, 3H), 7.24 - 7.20 (m, 1H), 7.10 - 7.07 (m, 2H), 5.49 - 5.42 (m, 1H), 3.82 (s, 3H), 1.55 (d, *J* = 7.1, 3H); ^{13}C NMR (100 MHz, DMSO-d_6): δ: 166.1, 160.2, 156.6, 153.7, 151.1, 145.3, 128.8 (2C), 127.1, 126.5 (2C), 126.2 (2C), 122.3, 115.2 (2C), 103.3, 97.3, 55.8, 49.5, 23.2; IR (neat, cm^{-1}): 3422, 2965, 1594, 1250, 1140, 1023, 778, 701; HRMS (APCI/ASAP, m/z): 346.1549 (calcd. $C_{21}H_{20}N_3O_2$, 346.1556, $[M+H]^+$).

4.10.2 (*R*)-6-Phenyl-*N*-(1-phenylethyl)furo[2,3-*d*]pyrimidin-4-amine (6b)

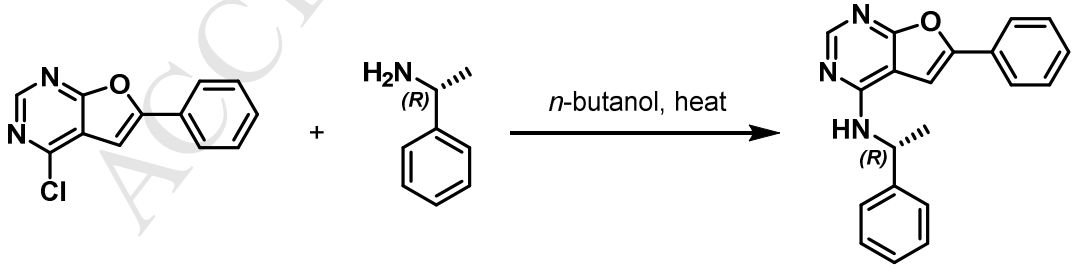

The synthesis was performed as described in Section 4.10 starting with **5b** (150 mg, 0.65 mmol). Silica-gel column chromatography (EtOAc/*n*-pentane 8/2, R_f = 0.39) gave 152 mg, (0.483 mmol, 74%) of **6b** as a white solid, mp 128 - 131 ˚C; HPLC purity: 98%, t_R = 30.4 min; $[\alpha]_D^{20}$ = -252.1 (c 0.85, DMSO); ^{1}H NMR (400 MHz, DMSO-d_6) δ: 8.35 - 8.33 (m, 1H), 8.21 (s, 1H), 7.81 - 7.78 (m, 2H), 7.54 - 7.50 (m, 3H), 7.44 - 7.39 (m, 3H), 7.35 - 7.31 (m, 2H), 7.24 - 7.20 (m, 1H), 5.51 - 5.44 (m, 1H), 1.55 (d, *J* = 7.0, 3H); ^{13}C NMR (100 MHz,

DMSO-d_6): δ: 165.8, 156.2, 153.7, 150.2, 144.7, 129.2 (2C), 128.8, 128.3 (2C), 126.7, 126.0 (2C), 124.1 (2C), 120.2, 102.5, 99.2, 49.3, 22.7; IR (neat, cm^{-1}): 3269, 3029, 2973, 1597, 755, 688; HRMS (APCI/ASAP, m/z): 316.1449 (calcd. $C_{20}H_{18}N_3O$, 316.1450, [M+H]+).

4.10.3 (*R*)-6-(4-Fluorophenyl)-*N*-(1-phenylethyl)furo[2,3-*d*]pyrimidin-4-amine (6c)

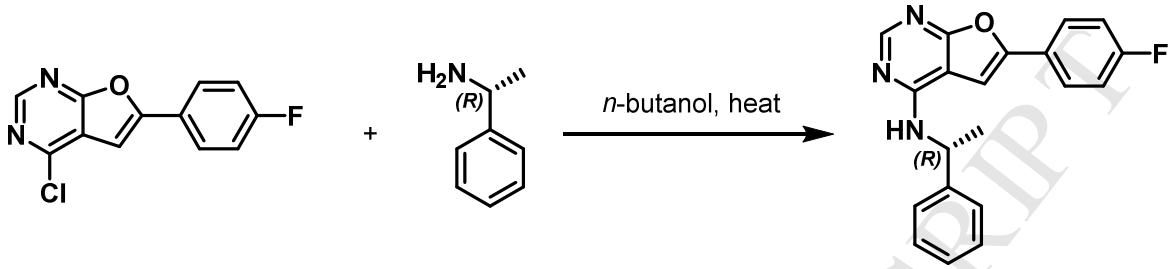

The synthesis was performed as described in Section 4.10 starting with **5c** (150 mg, 0.603 mmol). Silica-gel column chromatography (EtOAc/*n*-pentane 1/1, R_f = 0.24) gave 148 mg (0.44 mmol, 73%) of **6c** as a white solid; mp 121 - 124 ˚C; HPLC purity: 98%, t_R = 30.9 min; $[\alpha]_D^{20}$ = -228.7 (c 1.14, DMSO); ^{1}H NMR (400 MHz, DMSO-d_6) δ: 8.35 - 8.33 (m, 1H), 8.20 (s, 1H), 7.85 - 7.81 (m, 2H), 7.46 - 7.42 (m, 3H), 7.38 - 7.31 (m 4H), 7.24 - 7.20 (m, 1H), 5.49 - 5.43 (m, 1H), 1.55 (d, *J* = 7.0, 3H); ^{13}C NMR (100 MHz, DMSO-d_6) δ: 165.8, 162.2 (d, *J* = 246.6), 156.2, 153.7, 149.4, 144.7, 128.3 (2C), 126.7, 126.4 (d, *J* = 8.2, 2C), 126.0 (2C), 125.9, 116.3 (d, *J* = 22.1, 2C), 102.5, 99.0, 49.3, 22.6; IR (neat, cm^{-1}): 3269, 2973, 1593, 1499, 698; HRMS (APCI/ASAP, m/z): 334.1356 (calcd. $C_{20}H_{17}N_3OF$, 334.1356, [M+H]+).

4.10.4 (*R*)-6-(4-Bromophenyl)-*N*-(1-phenylethyl)furo[2,3-*d*]pyrimidin-4-amine (6d)

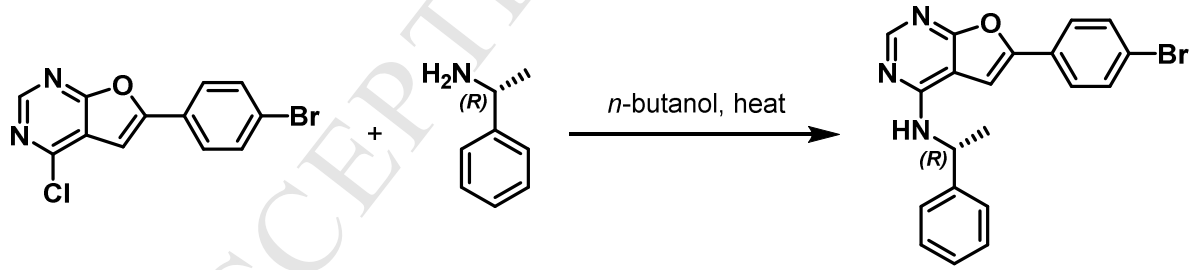

The synthesis was performed as described in Section 4.10 starting with **5d** (1.84 g, 5.95 mmol). Silica-gel column chromatography (CH_2Cl_2/MeOH 99/1, R_f = 0.38) followed by a re-slurry in Et_2O (15 mL) gave 1.85 g (4.71 mmol, 79%) of **6d** as a white solid, mp 157 - 158 ˚C; HPLC purity: 99%, t_R = 33.4 min; $[\alpha]_D^{20}$= -244.3 (1.00, DMSO); ^{1}H NMR (400 MHz, DMSO-d_6) δ: 8.39 - 8.37 (m, 1H), 8.21 (s, 1H), 7.74 - 7.69 (m, 4H), 7.54 (s, 1H), 7.44 - 7.42 (m, 2H), 7.34 - 7.31 (m, 2H), 7.24 - 7.20 (m, 1H), 5.50 - 5.43 (m, 1H), 1.55 (d, *J* = 7.0, 3H); ^{13}C NMR (100 MHz, DMSO-d_6) δ: 165.9, 156.2, 154.0, 149.1, 144.6, 132.2 (2C), 128.3 (2C), 126.7, 126.0 (5C), 121.7, 102.5, 100.0, 49.3, 22.6; IR (neat, cm^{-1}): 3412, 2969, 1595, 1479, 773; HRMS (APCI/ASAP, m/z): 394.0550 (calcd. $C_{20}H_{17}N_3OBr$, 394.0555, $[M+H]^+$).

4.10.5 (*R*)-4-(4-((1-phenylethyl)amino)furo[2,3-*d*]pyrimidin-6-yl)benzonitrile (6e)

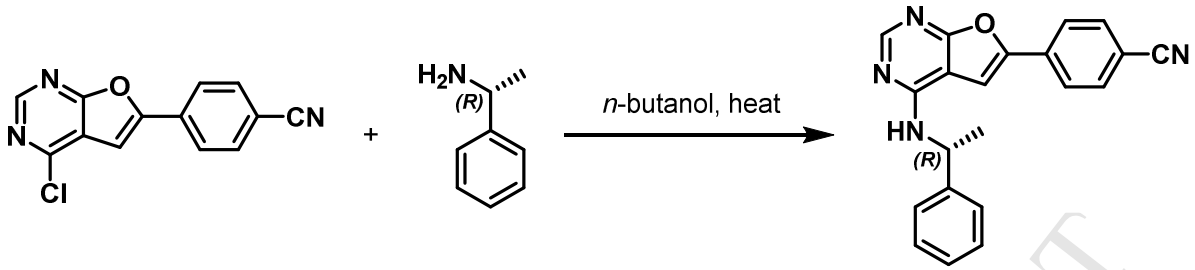

Compound **6e** was prepared as described in section 4.10 starting with **5e** (125 mg, 0.49 mmol). Silica-gel column chromatography (EtOAc/*n*-pentane, 1/1, R_f = 0.51) yielded 404 mg (1.12 mmol, 73%) of a white solid; mp 163 - 176 °C; HPLC purity: 99%, t_R = 23.9 min; $[\alpha]_D^{20}$= -205.2 (c 0.96, DMSO); ^{1}H NMR (400 MHz, DMSO-d_6) δ: 8.49 (d, *J* = 7.8, 1H), 8.24 (s, 1H), 7.94 - 7.90 (m, 4H), 7.70 (s, 1H), 7.42 (d, *J* = 7.2, 2H), 7.33 (t, *J* = 7.8, 2H), 7.22 (t, *J* = 7.3, 1H), 5.51 - 5.44 (m, 1H), 1.55 (d, *J* = 7.0, 3H); ^{13}C NMR (100 MHz, DMSO-d_6) δ: 166.2, 156.4, 154.6, 148.2, 144.5, 133.2, 133.1 (2C), 129.9, 128.3 (2C), 126.7 (2C), 126.0, 124.5 (2C), 118.6, 110.5, 102.6, 49.3, 22.5; IR (neat, cm^{-1}): 3360, 3056, 3028, 2977, 2927, 2227, 1594, 1493, 1309, 1138, 925, 945, 779, 696; HRMS (APCI/ASAP, m/z): 341.1400 (calcd. $C_{21}H_{17}N_4O$, 341.1402, $[M+H]^+$).

4.10.6 (*R*)-6-(3-Methoxyphenyl)-*N*-(1-phenylethyl)furo[2,3-*d*]pyrimidin-4-amine (6f)

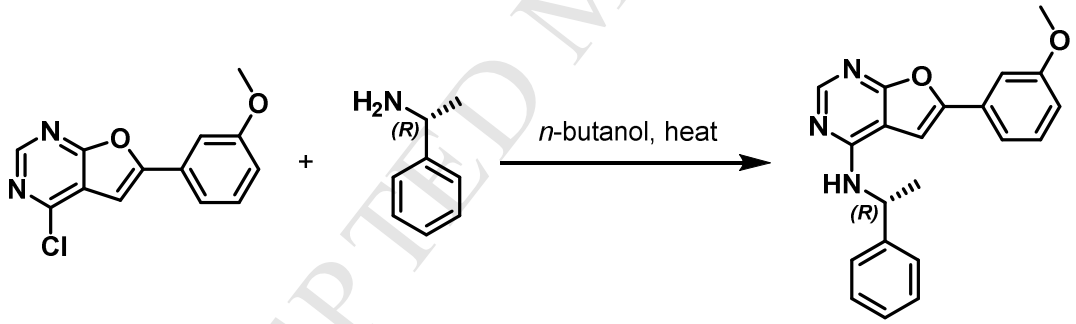

Compound **6f** was prepared as described in section 4.10 starting with **5f** (300 mg, 1.15 mmol). Silica-gel column chromatography (*n*-pentane/EtOAc, 3/2, R_f = 0.36) gave 323 mg (0.94 mmol, 81%) of **6f** as a white solid; mp 131 - 133 °C; HPLC purity: 98%, t_R = 30.7 min; $[\alpha]_D^{20}$ = -267.4 (c 1.04, DMSO); ^{1}H NMR (400 MHz, DMSO-d_6) δ: 8.35 - 8.33 (m, 1H), 8.21 (s, 1H), 7.51 (s, 1H), 7.44 - 7.41 (m, 3H), 7.38 - 7.28 (m, 4H), 7.24 - 7.20 (m, 1H), 6.99 - 6.97 (m, 1H), 5.50 - 5.43 (m, 1H), 3.85 (s, 3H), 1.55 (d, *J* = 7.0, 3H); ^{13}C NMR (100 MHz, DMSO-d_6) δ: 165.8, 159.7, 156.2, 153.8, 150.1, 144.7, 130.49, 130.44, 128.3 (2C), 126.7, 126.0 (2C), 116.5, 114.8, 108.9, 102.5, 99.6, 55.2, 49.3, 22.7; IR (neat, cm^{-1}): 3422, 2965, 1594, 1250, 1140, 1023, 778, 701; HRMS (APCI/ASAP, m/z): 346.1552 (calcd. $C_{21}H_{20}N_3O_2$, 346.1556, $[M+H]^+$).

4.10.7 (*R*)-6-(2-Methoxyphenyl)-*N*-(1-phenylethyl)furo[2,3-*d*]pyrimidin-4-amine (6g)

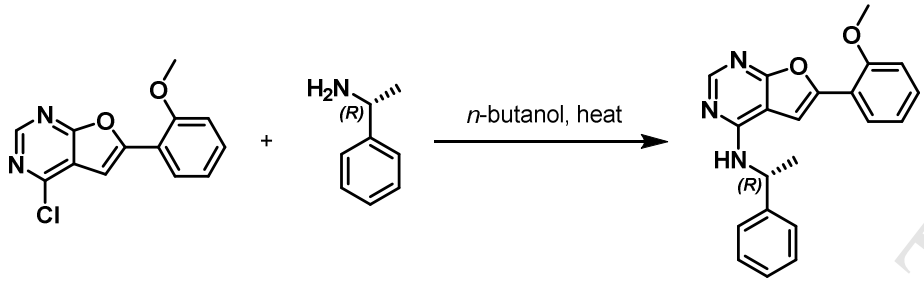

Compound **6g** was prepared as described in section 4.10 starting with **5g** (338 mg, 1.31 mmol. Silica-gel column chromatography (EtOAc, R_f = 0.60) gave 381 mg (1.10 mmol, 85%) of **6g** as a white solid; mp 107 - 110 °C ; HPLC purity: 99%, t_R = 30.8 min; $[\alpha]_D^{20}$ = -296.6 (c 1.00, DMSO-d_6); ^{1}H NMR (400 MHz, DMSO-d_6) δ: 8.36 - 8.34 (m, 1H), 8.20 (s, 1H), 7.87-7.84 (m, 1H), 7.67 (s, 1H), 7.45 - 7.42 (m, 2H), 7.41 - 7.37 (m, 1H), 7.35 - 7.31 (m, 2H), 7.25-7.20 (m, 2H), 7.12 - 7.08 (m, 1H), 5.53 - 5.46 (m, 1H), 4.02 (s, 3H), 1.56 (d, *J* = 7.0, 3H); ^{13}C NMR (100 MHz, DMSO-d_6) δ: 165.4, 156.5 (2C), 154.1, 147.3, 145.3, 130.1, 128.8 (2C), 127.1, 126.5 (2C), 126.3, 121.3, 118.2, 113.5, 112.3, 104.1, 56.2, 49.6, 23.1; IR (neat, cm^{-1}): 3258, 2971, 1593, 749, 698; HRMS (APCI/ASAP, m/z): 346.1551 (calcd. $C_{21}H_{20}N_3O_2$, 346.1556, $[M+H]^+$).

4.11 Post modifications

4.11.1 (*R*)-4-(4-((1-Phenylethyl)amino)furo[2,3-*d*]pyrimidin-6-yl)phenol (6h)

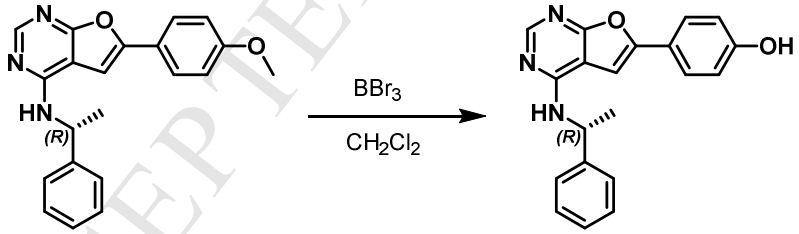

(*R*)-4-(4-((1-Phenylethyl)amino)furo[2,3-*d*]pyrimidin-6-yl)phenol (**6a**) was dissolved in dry CH_2Cl_2 (2 mL) under nitrogen atmosphere. BBr_3 (0.17 mL, 1.8 mmol) in dry CH_2Cl_2 (1.5 mL) was added drop wise at 0 ˚C over 1 h using a syringe pump. Then the mixture was allowed to react at rt for 24 h. The reaction was quenched by addition of water (10 mL), and the mixture was extracted with EtOAc (3 × 25 mL). The combined organic phase was washed with brine (15 mL), dried over Na_2SO_4 and concentrated *in vacuo*. The crude product was purified by silica-gel column chromatography (EtOAc/*n*-pentane, 8/2, R_f = 0.49). The product was further crystallised from diethyl ether (2 mL) by slowly adding *n*-pentane (30 mL). Evaporation and concentration *in vacuo* gave 114 mg (0.343 mmol, 80%) of **6g** as a white solid; mp 134 -136 °C; HPLC purity: 96%, t_R = 26.3 min; $[\alpha]_D^{20}$ = -269.4 (c 0.59, DMSO); ^{1}H NMR (400 MHz, DMSO-d_6) δ: 9.88 (s, 1H), 8.23 - 8.21 (m, 1H), 8.16 (s, 1H), 7.62 - 7.60 (m, 2H), 7.43 - 7.41 (m, 2H), 7.33 - 7.31 (m, 2H), 7.25 - 7.19 (m, 2H), 6.91 - 6.89 (m, 2H),

5.49 - 5.42 (m, 1H), 1.54 (d, *J* = 7.0, 3H); ^{13}C NMR (100 MHz, DMSO-d_6) δ: 165.5, 158.2, 155.9, 153.0, 151.1, 144.8, 128.3 (2C), 126.7, 126.0 (2C), 125.9 (2C), 120.3, 116.0 (2C), 102.7, 96.3, 49.2, 22.7; IR (neat, cm^{-1}): 3289, 3061, 1601, 698; HRMS (APCI/ASAP, m/z): 332.1396 (calcd. $C_{20}H_{18}N_3O_2$, 332.1399, $[M+H]^+$).

4.11.2 (*R*)-3-(4-((1-Phenylethyl)amino)furo[2,3-*d*]pyrimidin-6-yl)phenol (6i)

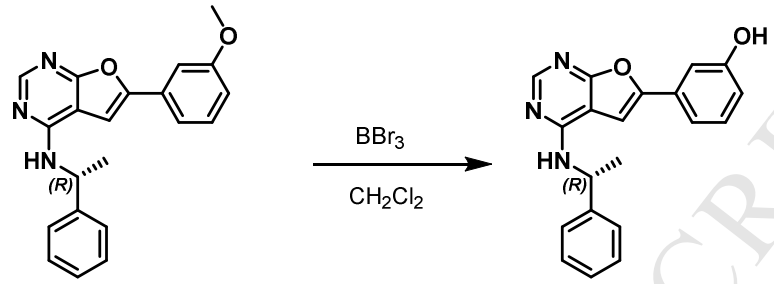

Compound **6i** was prepared as described in Section 3.8.1, but starting with compound **6f** (150 mg, 0.434 mmol). Silica-gel column chromatography (EtOAc/*n*-pentane 1/1, R_f = 0.41) and crystallisation from diethyl ether/*n*-pentane gave 114 mg (0.354 mmol, 82%) of **6i** as a white solid; mp 130 - 132 °C; HPLC purity: 96%, t_R = 26.6 min; $[\alpha]_D^{20}$ = -222.2 (c 1.03, DMSO); ^{1}H NMR (400 MHz, DMSO-d_6) δ: 9.74 (s, 1H), 8.32 - 8.31 (m, 1H), 8.20 (s, 1H), 7.43 - 7.41 (m, 3H), 7.34 - 7.29 (m, 3H), 7.24 - 7.20 (m, 2H), 7.17 - 7.16 (m, 1H), 6.81 - 6.79 (m, 1H), 5.50 - 5.43 (m, 1H), 1.55 (d, *J* = 7.0, 3H); ^{13}C NMR (100 MHz, DMSO-d_6) δ: 165.7, 157.9, 156.2, 153.7, 150.3, 144.7, 130.4, 130.3, 128.3 (2C), 126.7, 126.0 (2C), 115.9, 115.0, 110.6, 102.5, 99.0, 49.3, 22.6; IR (neat, cm^{-1}): 3294, 2973, 1602, 1454, 775; HRMS (APCI/ASAP, m/z): 332.1399 (calcd. $C_{20}H_{18}N_3O_2$, 332.1399, $[M+H]^+$).

4.11.3 (*R*)-2-(4-((1-Phenylethyl)amino)furo[2,3-*d*]pyrimidin-6-yl)phenol (6j)

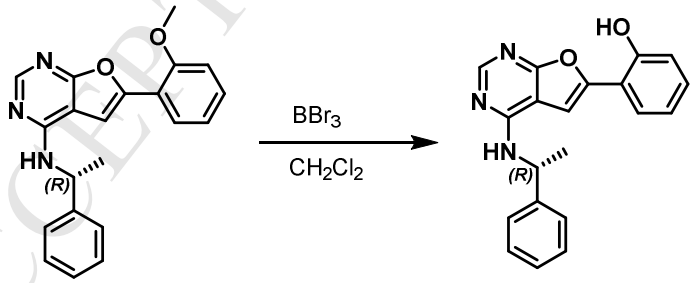

Compound **6j** was prepared as described in Section 3.8.1, but starting with compound **6g** (150 mg, 0.434 mmol). Purification by silica-gel column chromatography (EtOAc/*n*-pentane 1/1, R_f = 0.45), and precipitation from diethyl ether/n-pentane gave 110 mg (0.331 mmol, 76%) of **6j** as a white solid; mp 156 - 158 °C; HPLC purity: 96%, t_R = 27.5 min; $[\alpha]_D^{20}$ = -322.5 (c 1.03, DMSO); ^{1}H NMR (400 MHz, DMSO-d_6) δ: 10.47 (s, 1H), 8.39-8.37 (m, 1H), 8.17 (s, 1H), 7.78 - 7.76 (m, 1H), 7.70 (s, 1H), 7.43 - 7.41 (m, 2H), 7.34 - 7.30 (m, 2H), 7.23 - 7.19 (m, 2H), 7.04 - 7.02 (m, 1H), 6.96 - 6.92 (m, 1H), 5.49 - 5.43 (m, 1H), 1.54 (d, *J* = 7.1, 3H); ^{13}C NMR (100 MHz, DMSO-d_6) δ: 165.3, 156.6, 155.0, 153.8, 148.0, 145.4, 129.3, 128.7 (2C), 127.1, 126.5 (2C), 126.1, 120.1, 116.7, 103.5, 49.7, 23.1; IR (neat, cm^{-1}): 3301,

3054, 1639, 702; HRMS (APCI/ASAP, m/z): 332.1399 (calcd. $C_{20}H_{18}N_3O_2$, 332.1399, $[M+H]^+$).

4.11.4 (*R*)-*N*-(1-Phenylethyl)-6-(4-vinylphenyl)furo[2,3-d]pyrimidin-4-amine (6k)

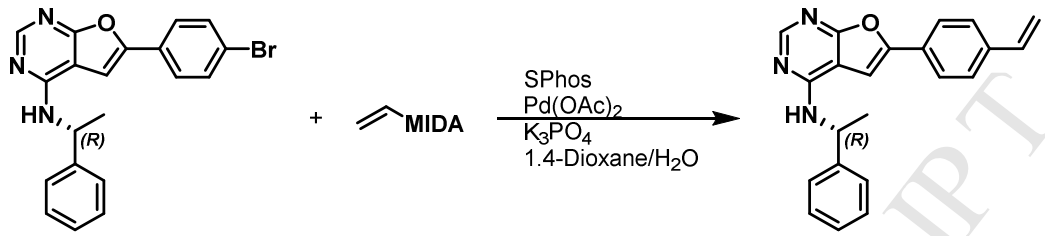

(*R*)-6-(4-Bromophenyl)-*N*-(1-phenylethyl)furo[2,3-*d*]pyrimidin-4-amine (**6d**) (786 mg, 2.00 mmol) was mixed with, vinyl MIDA boronate (402 mg, 2.2 mmol, 1.1 eq.), SPhos (82 mg, 0.2 mmol, 0.1 eq.), $Pd(OAc)_2$ (22 mg, 0.1 mmol, 0.05 eq.), K_3PO_4 (2.54 g, 12 mmol, 6 eq.) and a degassed solution 1,4-dioxane/water (5/2) (15 mL) under N_2 atmosphere. The reaction mixture was stirred for 3 hours at 95 °C under an N_2-atmosphere, diluted with CH_2Cl_2 (50 mL), cooled to 20 °C and filtered. The filtrate was evaporated to dryness. The residue was dissolved in CH_2Cl_2 (100 mL) and washed with water (2 × 50 mL) and brine (50 mL). The organic phase was dried over Na_2SO_4 and evaporated. The crude product was purified by silica-gel chromatography (CH_2Cl_2/MeOH, 99/1→98/2, R_f = 0.53 (CH_2Cl_2/MeOH, 94/6)) and gave 633 mg (1.85 mmol, 93 %) of **6k** as white solid; mp 70 - 71 °C, HPLC purity: 97%, t_R = 30.1 min; $[\alpha]_D^{20}$ = - 318.2 (c 1.00, DMSO); ^{1}H NMR (400 MHz, $CDCl_3$) δ: 8.38 (s, 1H), 7.72 (d, *J* = 8.3, 2H), 7.47 - 7.41 (m, 4H), 7.36 (t, *J* = 7.5, 2H), 7.29 (t, *J* = 6.9, 1H), 6.78 (s, 1H), 6.72 (dd, *J* = 17.6, 10.9, 1H), 5.80 (d, *J* = 17.6, 1H), 5.45 (br. s, 2H), 5.30 (d, *J* = 11.2, 1H), 1.68 (d, *J* = 6.6, 3H); ^{13}C NMR (100 MHz, $CDCl_3$) δ: 166.8, 156.6, 153.9, 152.1, 143.5, 138.2, 136.2, 129.0, 128.7 (2C), 127.7, 126.8, 126.13 (2C), 124.9 (2C), 114.8 (2C), 103.1, 97.3, 50.96, 22.9; IR (neat, cm^{-1}): 3265, 3059, 2974, 2927, 1583, 1493, 1448, 1352, 1299, 1138, 781; HRMS (APCI/ASAP, m/z): 342.1602 (calcd. for $C_{22}H_{20}N_3O$: 342.1606) $[M+H]^+$.

4.11.5 (*R*)-N^1,N^1-Dimethyl-N^2-(4-(4-((1-phenylethyl)amino)furo[2,3-*d*]pyrimidin-6-yl)phenyl)ethane-1,2-diamine (6l)

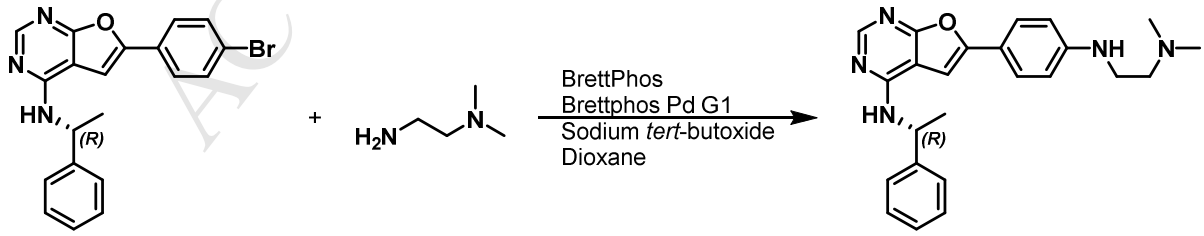

(*R*)-6-(4-Bromophenyl)-*N*-(1-phenylethyl)furo[2,3-*d*]pyrimidin-4-amine (**6d**) (50.1 mg, 0.127 mmol) was mixed with N^1,N^1-dimethylethane-1,2-diamine (17 µL, 0.152 mmol, 1.2 eq.), BrettPhos Pd G1 (2.03 mg, 2.54 µmol, 2 mol%), BrettPhos (1.36 mg, 2.54 µmol, 2 mol%) and NaO*t*-Bu (24 mg, 0.254 mmol, 2 eq.) and 1,4-dioxane (1 mL) under N_2 atmosphere. The

reaction mixture was stirred for 3h at 90 °C under an N_2-atmosphere. The reaction mixture was evaporated to dryness, extracted with EtOAc (2 x 15 mL), washed with water (20 mL) and saturated aq. NaCl solution (10 mL), dried over Na_2SO_4 and concentrated *in vacuo*. The crude product was purified by silica-gel chromatography (EtOAc/MeOH, 100/0→85/15, R_f = 0.05 (EtOAc/MeOH 85/15)) and gave 33.4 mg (0.084 mmol, 66%) of **6l** as a yellow solid; mp 96 - 98 °C, $[\alpha]_D^{20}$ = - 298.6 (c 0.49, DMSO), HPLC purity: 97%, t_R = 21.5 min; ^{1}H NMR (400 MHz, DMSO-d_6) δ: 8.14 (d, *J* = 8.1, 1H), 8.11 (s, 1H), 7.52 - 7.49 (m, 2H), 7.43 - 7.41 (m, 2H), 7.33 - 7.30 (m, 2H), 7.23 - 7.19 (m, 1H), 7.11 (s, 1H), 6.70 - 6.68 (m, 2H), 5.91 (t, *J* = 5.4, 1H), 5.47 - 5.40 (m, 1H), 3.15 (q, *J* = 6.6, 2H), 2.45 (t, *J* = 6.6, 2H), 2.19 (s, 6H), 1.53 (d, *J* = 7.0, 3H); IR (neat, cm^{-1}): 3278, 2966, 2810, 1605, 1509, 1468, 1140, 699; ^{13}C NMR (100 MHz, DMSO-d_6) δ: 165.4, 155.7, 152.5, 152.0, 149.5, 145.0, 128.3 (2C), 126.7, 126.1 (2C), 125.5 (2C), 116.6, 112.2 (2C), 103.0, 94.5, 57.8, 49.3, 45.3 (2C), 40.6, 22.8; HRMS (APCI/ASAP, m/z): 402.2292 (calcd. $C_{24}H_{28}N_5O$, 402.2294, $[M+H]^+$).

4.11.6 (*R*)-6-(4-((2-Morpholinoethyl)amino)phenyl)-*N*-(1-phenylethyl)furo[2,3-*d*]pyrimidin-4-amine (6n)

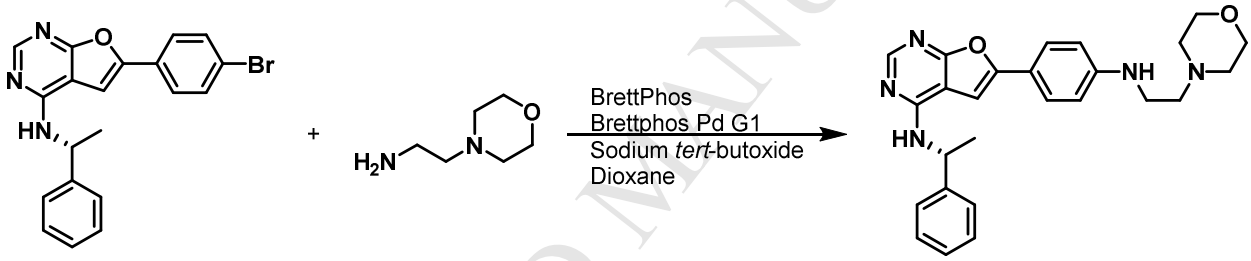

(*R*)-6-(4-Bromophenyl)-*N*-(1-phenylethyl)furo[2,3-*d*]pyrimidin-4-amine (**6d**) (101 mg, 0.256 mmol) was mixed with 2-morpholinoethan-1-amine (40 µL, 0.307 mmol, 1.2 eq.), BrettPhos Pd G1 (4.10 mg, 5.12 µmol, 2 mol%), BrettPhos (2.72 mg, 5.12 µmol, 2 mol%) and NaO*t*-Bu (49 mg, 0.512 mmol, 2 eq.) and 1,4-dioxane (1.5 mL) under N_2 atmosphere. The reaction mixture was stirred for 2h at 100 °C under an N_2-atmosphere. The reaction mixture was evaporated to dryness, extracted with EtOAc (3 x 20 mL), washed with water (20 mL) and saturated aq. NaCl solution (10 mL), dried over Na_2SO_4 and concentrated *in vacuo*. The crude product was purified by silica-gel chromatography (EtOAc, R_f = 0.10) and gave 90.1 mg (0.205 mmol, 80%) of **6n** as a yellow solid; mp 103 - 104 °C, $[\alpha]_D^{20}$ = - 287.0 (c 0.99, DMSO), HPLC purity: 97%, t_R = 26.3 min; ^{1}H NMR (400 MHz, DMSO-d_6) δ: 8.13 - 8.11 (m, 2H), 7.52 - 7.50 (m, 2H), 7.43 - 7.41 (m, 2H), 7.33 - 7.30 (m, 2H), 7.23 - 7.19 (m, 1H), 7.11 (s, 1H), 6.70 - 6.68 (m, 2H), 5.95 (t, *J* = 5.4, 1H), 5.48 - 5.41 (m, 1H), 3.59 (t, *J* = 4.5, 4H), 3.19 (q, *J* = 6.3, 2H), 2.51 (t, *J* = 6.6, 2H), 2.43 (t, *J* = 4.5, 4H), 2.19 (s, 6H), 1.53 (d, *J* = 7.0, 3H); ^{13}C NMR (100 MHz, DMSO-d_6) δ: 165.3, 155.7, 152.5, 151.9, 149.4, 144.9, 128.3 (2C), 126.6, 126.0 (2C), 125.5 (2C), 116.6, 112.2 (2C), 102.9, 94.5, 66.2 (2C), 59.8, 57.0, 53.4 (2C), 49.2, 22.8; IR (neat, cm^{-1}): 3283, 2930, 2847, 1605, 1509, 1478, 1136, 698; HRMS (APCI/ASAP, m/z): 444.2393 (calcd. $C_{26}H_{30}N_5O_2$, 444.2400, $[M+H]^+$).

4.11.7 (*R*)-*N*-(1-Phenylethyl)-6-(4-((2-(piperidin-1-yl)ethyl)amino)phenyl)furo[2,3-*d*]pyrimidin-4-amine (6l)

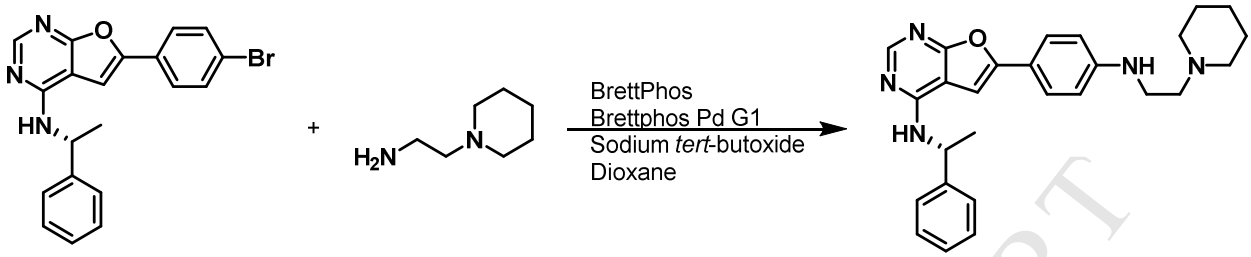

(*R*)-6-(4-Bromophenyl)-*N*-(1-phenylethyl)furo[2,3-*d*]pyrimidin-4-amine (**6d**) (100 mg, 0.254 mmol) was mixed with 2-(piperidin-1-yl)ethan-1-amine (43 µL, 0.304 mmol, 1.2 eq.), BrettPhos Pd G1 (4.05 mg, 5.07 µmol, 2 mol%), BrettPhos (2.72 mg, 5.07 µmol, 2 mol%), NaO*t*-Bu (49 mg, 0.507 mmol, 2 eq.) and 1,4-dioxane (1.5 mL) under N_2 atmosphere. After cooling to rt the reaction mixture was stirred for 2h at 100 °C under an N_2-atmosphere. The reaction mixture was evaporated to dryness, extracted with EtOAc (2 x 30 mL), washed with water (20 mL) and saturated aq. NaCl solution (20 mL), dried over Na_2SO_4 and concentrated *in vacuo*. The crude product was purified by silica-gel chromatography (EtOAc, R_f = 0.09) and gave 98.3 mg (0.224 mmol, 88%) of **6l** as a yellow solid; mp 100 - 102 °C, $[\alpha]_D^{20}$ = - 257.3 (c 1.01, DMSO), HPLC purity: 98%, t_R = 21.5 min; ^{1}H NMR (400 MHz, DMSO-d_6) δ: 8.13 - 8.11 (m, 2H), 7.51 - 7.49 (m, 2H), 7.43 - 7.41 (m, 2H), 7.33 - 7.30 (m, 2H), 7.23 - 7.19 (m, 1H), 7.11 (s, 1H), 6.70 - 6.67 (m, 2H), 5.91 (t, *J* = 5.4, 1H), 5.48 - 5.41 (m, 1H), 3.17 (q, *J* = 6.3, 2H), 2.47 (t, *J* = 6.6, 2H), 2.38 (t, *J* = 4.5, 4H), 1.54 - 1.48 (m, 7H), 1.41 - 1.37 (m, 2H); ^{13}C NMR (100 MHz, DMSO-d_6) δ: 165.3, 155.7, 152.5, 151.9, 149.5, 144.9, 128.3 (2C), 126.6, 126.0 (2C), 125.5 (2C), 116.5, 112.2 (2C), 103.0, 94.5, 59.8, 57.4, 54.2 (2C), 49.2, 25.6 (2C), 24.1, 22.8; IR (neat, cm^{-1}): 3304, 2956, 2857, 2810, 1595, 1509, 1114, 699; HRMS (APCI/ASAP, m/z): 444.2602 (calcd. $C_{27}H_{32}N_5O$, 444.2607, $[M+H]^+$).

4.12 Substitution at C-4 with other amines

4.12.1 (*S*)-2-((6-(4-Methoxyphenyl)furo[2,3-*d*]pyrimidin-4-yl)amino)-2-phenylethan-1-ol (7a)

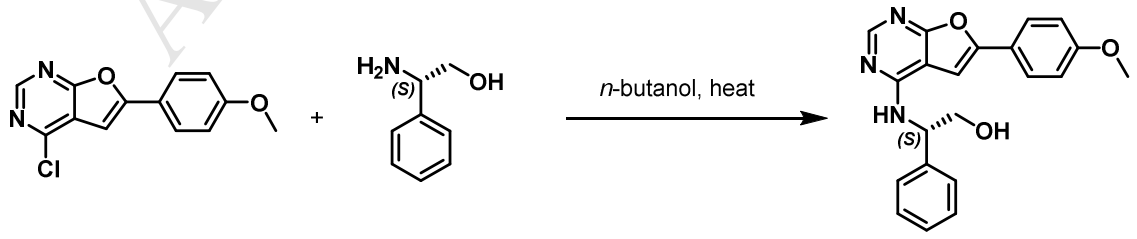

Compound **7a** was prepared as described in Section 4.10 starting with 4-chloro-6-(4-methoxyphenyl)furo[2,3-*d*]pyrimidine (**5a**) (300 mg, 1.15 mmol) and (*S*)-2-amino-2-

phenylethan-1-ol (474 mg, 3.45 mmol). Column chromatography on silica-gel (EtOAc/*n*-pentane, 9/1, R_f = 0.44) gave the product **7a** in 352 mg (0.975 mmol, 85%) as a white solid; mp 193 - 196 °C, $[\alpha]_D^{20}$ = - 226.6 (c 0.99, DMSO), HPLC purity: 98%, t_R = 22.8 min; ^{1}H NMR (400 MHz, DMSO-d_6) δ: 8.22 - 8.20 (m, 1H), 8.17 (s, 1H), 7.74 - 7.71 (m, 2H), 7.45 - 7.43 (m, 2H), 7.39 (s, 1H), 7.34 - 7.30 (m, 2H), 7.24 - 7.21 (m, 1H), 7.09 - 7.07 (m, 2H), 5.44 - 5.38 (m, 1H), 5.03 (t, *J* = 5.6, 1H) 3.21 (s, 3H), 3.77-3.72 (m, 2H); ^{13}C NMR (100 MHz, DMSO-d_6) δ: 166.1, 160.2, 157.1, 153.6, 151.1, 141.7, 128.6 (2C), 127.5 (2C), 127.3, 126.2 (2C), 122.4, 115.2 (2C), 103.3, 97.8, 65.3, 56.9, 55.8; IR (neat, cm^{-1}): 3435, 2978, 1611, 1270, 1141, 1023, 751, 700; HRMS (APCI/ASAP, m/z): 362.1503 (calcd. $C_{21}H_{20}N_3O_3$, 362.1505, $[M+H]^+$).

4.12.2 (*S*)-2-Phenyl-2-((6-phenylfuro[2,3-*d*]pyrimidin-4-yl)amino)ethanol (7b)

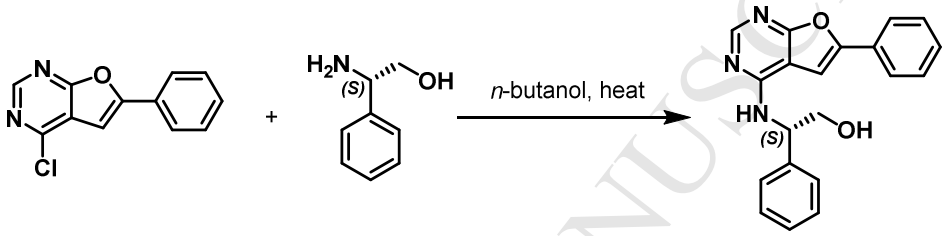

Compound **7b** was prepared as described in Section 4.10 starting with 4-chloro-6-phenylfuro[2,3-*d*]pyrimidine (230 mg, 1.00 mmol) and (*S*)-2-amino-2-phenylethanol (411 mg, 3.00 mmol, 3 eq.) Column chromatography on silica-gel (*n*-pentane/EtOAc, 1/1, R_f = 0.28) gave 270 mg (0.82 mmol, 82 %) of **7b** as a white solid, mp 108 - 109 °C, $[\alpha]_D^{20}$ = - 242.8 (c 1.00, DMSO), HPLC purity: 96%, t_R = 22.0 min; ^{1}H NMR (400 MHz, DMSO-d_6) δ: 8.20 (s, 1H), 7.80 (d, *J* = 7.3, 2H), 7.57 (s, 1H), 7.52 (t, *J* = 7.7, 2H), 7.48 - 7.38 (m, 3H), 7.33 (t, *J* = 7.6, 2H), 7.23 (t, *J* = 7.3, 1H), 5.42 (m, 1H), 5.04 (t, *J* = 5.6, 1H), 3.79 - 3.72 (m, 2H); ^{13}C NMR (100 MHz, DMSO-d_6) δ: 165.9, 156.9, 153.7, 150.2, 141.1, 129.2 (2C), 128.7 (2C), 128.2, 127.0, 126.9 (2C), 124.1 (2C), 102.7, 99.3, 64.8, 56.5; IR (neat, cm^{-1}): 3257, 3170, 3059, 3029, 2930, 2862, 1600, 1471, 1444, 1352 1333, 753; HRMS (ASAP)**:** m/z = 332.1403 (calcd. for $C_{20}H_{18}N_3O_2$: 332.1399) $[M+H]^+$.

4.12.3 (*S*)-4-(4-((2-Hydroxy-1-phenylethyl)amino)furo[2,3-*d*]pyrimidin-6-yl)phenol (7h)

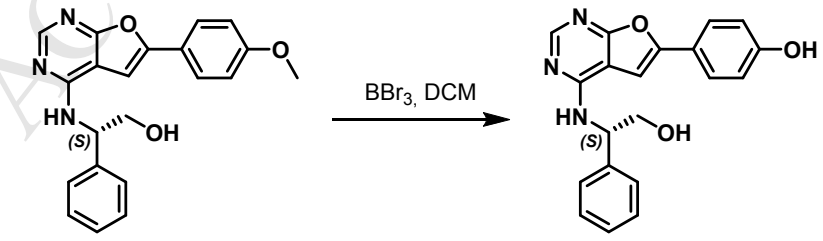

(*S*)-2-((6-(4-Methoxyphenyl)furo[2,3-*d*]pyrimidin-4-yl)amino)-2-phenylethan-1-ol (**7a**) (152 mg, 0.420 mmol) was dissolved in dry CH_2Cl_2 (4 mL) under nitrogen atmosphere. BBr_3 (4.15 mL, 4.15 mmol, 1M) in dry CH_2Cl_2 (4.5 mL) was added drop wise at -78 °C over 1 h using a syringe pump. Then the mixture was allowed to react at rt for 24 h. The reaction was

quenched by addition of water (10 mL), and the mixture was extracted with EtOAc (2 × 25 mL). The combined organic phase was washed with brine (15 mL), dried over Na_2SO_4 and concentrated *in vacuo*. Purification by silica-gel column chromatography (Et_2O/MeOH, 9/1, R_f = 0.60) gave 136 mg (0.394 mmol, 95%) of **7h** as a pale solid; mp 182 - 180 °C, HPLC purity: 97%, t_R = 19.1 min; ^{1}H NMR (400 MHz, DMSO-d_6) δ: 9.87 (s, 1H), 8.15 - 8.13 (m, 2H), 7.64 - 7.61 (m, 2H), 7.44 - 7.42 (m, 2H), 7.33 - 7.30 (m, 3H), 7.24 - 7.21 (m, 1H), 6.91 - 6.89 (m, 2H), 5.42 - 5.37 (m, 1H), 5.01 - 4.99 (m, 1H), 3.75 - 3.73 (m, 2H); ^{13}C NMR (100 MHz, DMSO-d_6) δ: 165.5, 158.2, 156.6, 152.9, 151.0, 141.3, 128.1 (2C), 127.0 (2C), 126.8, 125.9 (2C), 120.4, 116.0 (2C), 102.9, 96.4, 64.8, 59.7; IR (neat, cm^{-1}): 3285, 3162, 2942, 1610, 1472, 1361, 748; HRMS (APCI/ASAP, m/z): 348.1348 (calcd. $C_{20}H_{18}N_3O_3$, 348.1348, $[M+H]^+$).

4.12.4 *N*-Benzyl-6-(4-methoxyphenyl)furo[2,3-d]pyrimidin-4-amine (8a)

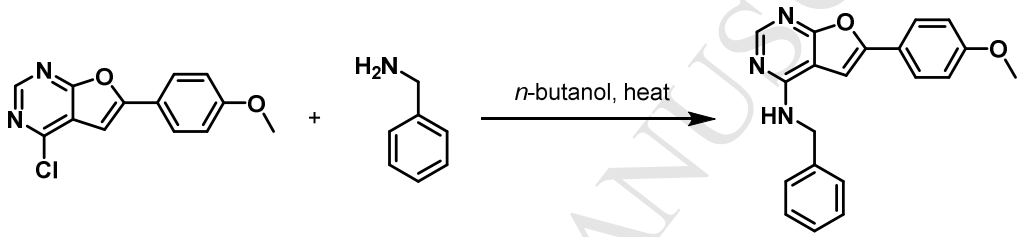

Compound **8a** was prepared as described in Section 4.10 starting with 4-chloro-6-(4-methoxyphenyl)furo[2,3-*d*]pyrimidine (**5a**) (350 mg, 1.34 mmol) and phenylmethanamine (432 mg, 4.03 mmol). Purification by silica-gel column chromatography (*n*-pentane/EtOAc, 1/1, R_f = 0.41) gave 396 mg (1.21 mmol, 89%) of **8a** as a white solid; mp 129 - 132 °C; HPLC purity: 97%, t_R = 26.0 min; ^{1}H NMR (400 MHz, DMSO-d_6) δ: 8.44 - 8.41 (m, 1H), 8.24 (s, 1H), 7.74 - 7.70 (m, 2H), 7.38 - 7.32 (m, 4H), 7.27 - 7.23 (m, 2H), 7.09 - 7.06 (m, 2H), 4.74 (d, *J* = 5.9, 2H), 3.81 (s, 3H); ^{13}C NMR (100 MHz, DMSO-d_6) δ: 165.6, 159.7, 156.8, 153.3, 150.6, 139.4, 128.4 (2C), 127.3 (2C), 126.9, 125.8 (2C), 121.8, 114.7 (2C), 102.7, 97.0, 55.3, 43.6; IR (neat, cm^{-1}): 3262, 2980, 1602, 750, 699; HRMS (APCI/ASAP, m/z): 332.1402 (calcd. $C_{20}H_{18}N_3O_2$, 332.1399, $[M+H]^+$).

4.12.5 *N*-Benzyl-6-phenylfuro[2,3-*d*]pyrimidin-4-amine (8b)

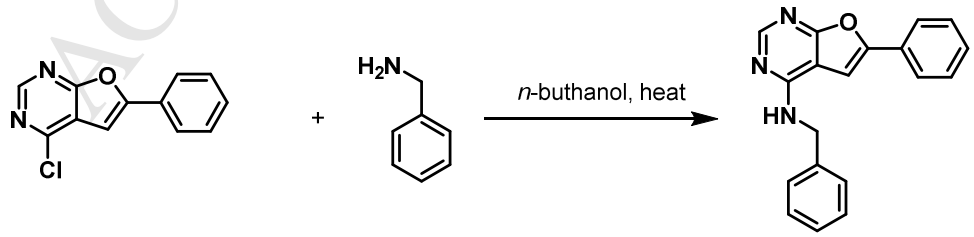

4-Chloro-6-phenylfuro[2,3-*d*]pyrimidine **(5b)** (230 mg, 1.00 mmol) and benzyl amine (268 mg, 2.50 mmol, 2.5 eq) were added to *i*-PrOH (10 mL) and the mixture was stirred for 6 h at 85 °C. After cooling to 20 °C, excess benzyl amine hydrochloride precipitated from solution as white crystals. The suspension was diluted with ethyl acetate (100 mL) and washed with water (2 × 50 mL) and brine (50 mL). The organic phase was dried over

anhydrous Na_2SO_4, filtered and concentrated. The crude product was purified by silica-gel chromatography (*n*-pentane/ EtOAc, 3/1→2/1, R_f = 0.60 (*n*-pentane/EtOAc 3/2)) and gave 271 mg (0.90 mmol, 90 %) of **8b** as a white solid; mp 187 - 188 °C; HPLC purity: 99%, t_R = 26.6 min; ^{1}H NMR (400 MHz, DMSO-d_6) δ: 8.50 (t, *J* = 5.8, 1H), 8.27 (s, 1H), 7.79 (d, *J* = 7.4, 2H), 7.50 (t, *J* = 7.7, 1H), 7.49 - 7.3 (m, 6H), 7.25 (t, *J* = 7.1, 1H), 4.75 (d, *J* = 5.9, 2H); ^{13}C NMR (100 MHz, DMSO-d_6) δ: 165.82, 157.00, 153.79, 150.34, 139.34, 129.16, 129.15, 128.71 (2C), 128.34 (2C), 127.35 (2C), 126.88, 124.11 (2C), 102.53, 98.96, 43.59; IR (neat, cm^{-1}) 3240,0, 3170.8, 3051.8, 2913.9, 1597.5, 1559.9, 1518.5, 1446.3, 751.9; HRMS (APCI/ASAP, m/z): 302.1292 (calculated for $C_{19}H_{16}N_3O$: 302.1293) $[M+H]^+$).

4.12.6 (*S*)-*N*-(2-Methoxy-1-phenylethyl)-6-(4-methoxyphenyl)furo[2,3-*d*]pyrimidin-4-amine (9a)

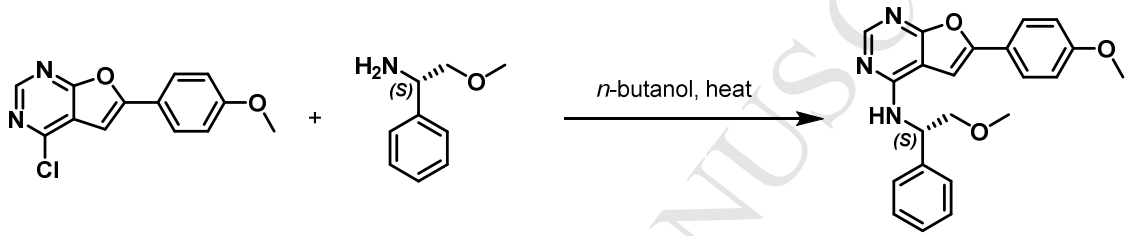

Compound **9a** was prepared as described in Section 4.10 starting with 4-chloro-6-(4-methoxyphenyl)furo[2,3-*d*]pyrimidine (**5a**) (400 mg, 1.53 mmol) and (*S*)-2-methoxy-1-phenylethan-1-amine (631 mg, 4.60 mmol). The reaction mixture was heated at 120 °C for 36 h. Column chromatography on silica-gel (EtOAc/*n*-pentane 1/1, R_f = 0.37) yielded 421 mg (1.12 mmol, 73%) of a pale yellow solid; mp 128 - 129 ˚C; HPLC purity: 99%, t_R = 24.3 min; $[\alpha]_D^{20}$ = - 260.7 (c 1.00, DMSO); ^{1}H NMR (400 MHz, DMSO-d_6) δ: 8.31 (d, *J* = 8.31, 1H), 8.19 (s, 1H), 7.74 (d, *J* = 8.8, 2H), 7.47 (d, *J* = 7.5, 2H), 7.39 (s, 1H), 7.34 (t, *J* = 7.7, 2H), 7.25 (t, *J* = 7.2, 1H), 7.09 (d, *J* = 8.9, 2H), 5.68-5.55 (m, 1H), 3.82 (s, 3H), 3.78 - 3.62 (m, 2H), 3.32 (s, 3H); ^{13}C NMR (100 MHz, DMSO-d_6) δ: 166.2, 160.2, 156.9, 153.6, 151.1, 141.1, 128.7 (2C), 127.6, 127.4 (2C), 126.2 (2C), 122.4, 115.2 (2C), 103.3, 97.7, 75.5, 58.6, 55.8, 53.8; IR (neat, cm^{-1}): 3285, 2927, 2890, 2830, 1600, 1499, 1245, 1167, 1021, 831, 781, 697; HRMS (APCI/ASAP, m/z): 376.1659 (calcd. $C_{22}H_{22}N_3O_3$, 376.1661, $[M+H]^+$).

4.12.7 (*S*)-*N*-(2-Methoxy-1-phenylethyl)-6-phenylfuro[2,3-*d*]pyrimidin-4-amine (9b)

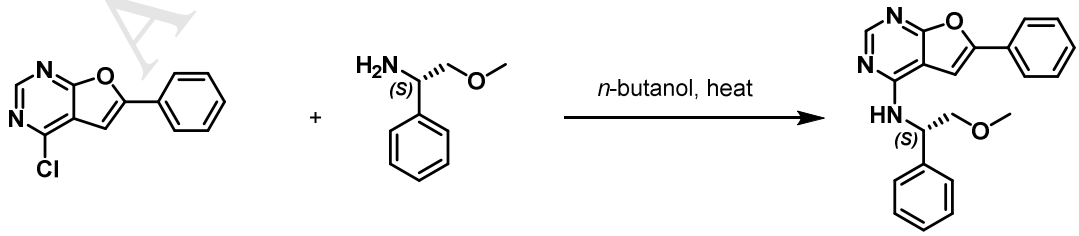

Compound **9b** was prepared as described in section 3.7 starting with 4-chloro-6-phenylfuro[2,3-*d*]pyrimidine (230 mg, 1.00 mmol) and (*S*)-2-methoxy-1-phenylethanamine (453 mg, 3.00 mmol, 3 eq.). Column chromatography on silica-gel (*n*-pentane/EtOAc,

3/1→2/1) gave 332 mg (0.96 mmol, 96 %) of **9b** as a white solid, R_f = 0.64 (*n*-pentane/ EtOAc, 1/1); mp 60 - 61 °C; $[\alpha]_D^{20}$ = - 215.8 (c 1.01, DMSO); HPLC**:** purity 98%, t_R = 25.8 min; ^{1}H NMR (400 MHz, DMSO-d_6) δ: 8.41 (d, *J* = 8.2, 1H), 7.21 (s, 1H), 7.80 (d, *J* = 7.3, 2H), 7.56 (s, 1H), 7.52 (t, *J* = 7.4, 2H), 7.47 (d, *J* = 7.4, 2H), 7.40 (t, *J* = 7.3, 1H), 7.34 (t, *J* = 7.4, 2H), 7.25 (t, *J* = 7.3, 1H), 5.57 - 5.68 (m, 1H), 3.61 - 3.78 (m, 2H), 3.32 (s, 3H); ^{13}C NMR (100 MHz, DMSO-d_6) δ: 168.87, 156.63, 153.67, 150.32, 140.55, 129.21, 129.19, 128.75 (2C), 128.28, 127.12 (2C), 126.95 (2C), 124.12 (2C), 102.69, 99.19, 74.92, 58.08, 53.35; IR (neat, cm^{-1}): 3283.1, 3059.7, 3028.6, 2919.5, 2849.5, 1595.8, 1489.8, 1465.8, 758. HRMS (ASAP): m/z = 346.1560 (calculated for $C_{21}H_{20}N_3O_2$: 346.1556) $[M+H]^+$.

4.12.8 (*R*)-6-(4-Methoxyphenyl)-*N*-(1-phenylpropyl)furo[2,3-*d*]pyrimidin-4-amine (10a)

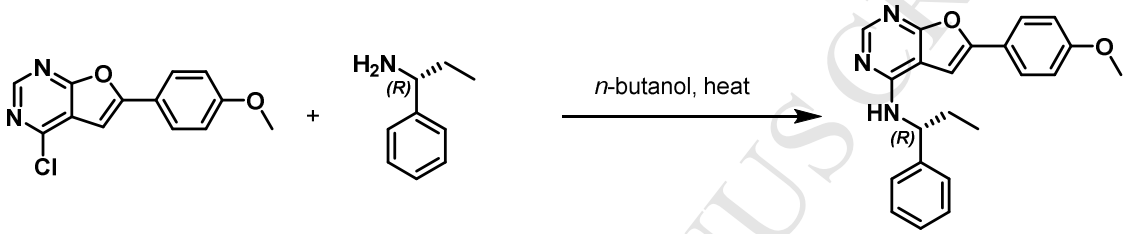

Compound **10a** was prepared as described in Section 4.10 starting with 4-chloro-6-(4-methoxyphenyl)furo[2,3-*d*]pyrimidine (**5a**) (400 mg, 1.53 mmol) and (*R*)-1-phenylpropan-1-amine (622 mg, 4.60 mmol). The reaction was heated at 140 ˚C for 23 h. Column chromatography on silica-gel (*n*-pentane/EtOAc 4/1, R_f = 0.25) yielded 404 mg (1.12 mmol, 73%) of **10a** as a white solid; mp 127 - 129 °C; HPLC purity: 99%, t_R = 20.6 min; $[\alpha]_D^{20}$ = - 253.5 (c 0.99, DMSO); ^{1}H NMR (400 MHz, DMSO-d_6) δ: 8.19 (d, *J* = 8.2, 1H), 8.17 (s, 1H), 7.72 (d, *J* = 8.8, 2H), 7.42 (d, *J* = 7.5, 2H), 7.35 (s, 1H), 7.32 (t, *J* = 7.7, 2H), 7.21 (t, *J* = 7.3, 1H), 7.07 (d, *J* = 8.7, 2H), 5.29 - 5.18 (m, 1H), 3.81 (s, 3H), 1.98 - 1.79 (m, 2H), 0.94 (t, *J* = 7.2, 3H); ^{13}C NMR (100 MHz, DMSO-d_6) δ: 166.1, 160.2, 156.9, 153.6, 150.9, 144.3, 128.7 (2C), 127.2, 127.0 (2C), 126.2 (2C), 122.4, 115.2 (2C), 103.2, 97.7, 56.0, 55.7, 29.9, 11.7; IR (neat, cm^{-1}): 3267, 2956, 2930, 1589, 1501, 1247, 1172, 1023, 831, 774, 701; HRMS (APCI/ASAP, m/z): 360.1708 (calcd. $C_{22}H_{22}N_3O_2$, 360.1712, $[M+H]^+$).

4.12.9 3-((6-(4-Methoxyphenyl)furo[2,3-*d*]pyrimidin-4-yl)amino)-3-phenylpropanamide (11a)

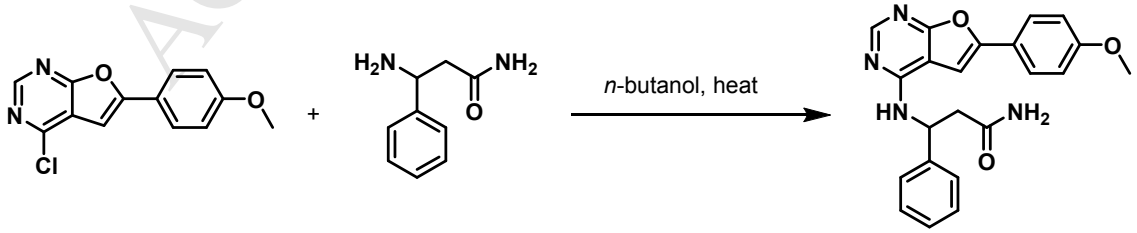

Compound **11a** was prepared as described in Section 4.10 starting with 4-chloro-6-(4-methoxyphenyl)furo[2,3-*d*]pyrimidine (**5a**) (180 mg, 0.69 mmol) and 3-amino-3-phenylpropanamide (340 mg, 2.07 mmol). The reaction mixture was heated at 100 °C for 45

h. Column chromatography on silica-gel (EtOAc, R_f = 0.19) yielded 103 mg (0.271 mmol, 39%) of **11a** as a white solid; mp. 221 - 230 °C; HPLC purity: 99%, t_R = 19.5 min; ^{1}H NMR (400 MHz, DMSO-d_6) δ: 8.29 (d, *J* = 8.4, 1H), 8.19 (s, 1H), 7.74 (d, *J* = 8.8, 2H), 7.45 (d, *J* = 7.6, 2H), 7.39 (s, 1H), 7.32 (t, *J* = 7.4, 2H), 7.30 (s, 1H), 7.22 (t, *J* = 7.2, 1H), 7.09 (d, *J* = 8.8, 2H), 6.84 (s, 1H), 5.83 - 5.74 (m, 1H), 3.82 (s, 3H), 2.77 - 2.65 (m, 2H); ^{13}C NMR (100 MHz, DMSO-d_6) δ: 171.8, 166.1, 160.2, 156.5, 153.7, 151.1, 143.6, 128.7 (2C), 127.3, 127.0 (2C), 126.2 (2C), 122.3, 115.2 (2C), 103.3, 97.5, 55.8, 51.5, 42.7; IR (neat, cm^{-1}): 3387, 3277, 3163, 2935, 2904, 2831, 1667, 1610, 1503, 1349, 1249, 1172, 1015, 777, 697; HRMS (APCI/ASAP, m/z): 389.1607 (calcd. $C_{22}H_{21}N_4O_3$, 389.1614, $[M+H]^+$).

4.12.10 (*R*)-3-((6-(4-Methoxyphenyl)furo[2,3-d]pyrimidin-4-yl)amino)-3-phenylpropan-1-ol (12a)

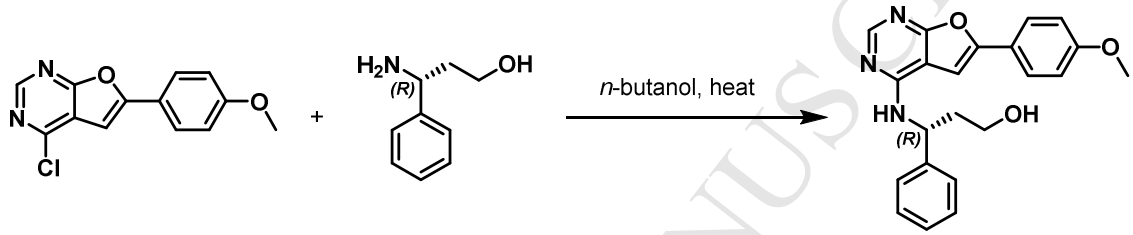

Compound **12a** was prepared as described in Section 4.10 starting with 4-chloro-6-(4-methoxyphenyl)furo[2,3-*d*]pyrimidine (**5a**) (301 mg, 1.15 mmol) and (*R*)-3-amino-3-phenylpropan-1-ol (501 mg, 3.45 mmol). Purification by silica-gel column chromatography (Et_2O/MeOH, 9/1, R_f = 0.63) and recrystallization from ACN gave 184 mg (0.495 mmol, 43%) of **12a** as a white solid; mp 211 - 212 °C; HPLC purity: 97%, t_R = 22.4 min; $[\alpha]_D^{20}$ = -204.6 (c 0.99, DMSO); ^{1}H NMR (400 MHz, DMSO-d_6) δ: 8.24 - 8.21 (m, 1H), 8.15 (s, 1H), 7.74 - 7.72 (m, 2H), 7.43 - 7.41 (m, 2H), 7.34 - 7.30 (m, 3H), 7.22 - 7.19 (m, 1H), 7.09 - 7.07 (m, 2H), 5.49 - 5.44 (m, 1H), 4.60 - 4.57 (m, 1H), 3.82 (s, 3H), 3.55 - 3.42 (m, 2H), 2.11 - 1.03 (m, 1H), 1.99 - 1.91 (m, 1H); ^{13}C NMR (100 MHz, DMSO-d_6) δ: 159.7, 156.5, 153.2, 150.5, 144.1 (2C), 128.3 (2C), 126.6, 126.4 (2C), 125.7 (2C), 121.9, 114.7 (2C), 97.1, 73.2, 57.8, 55.3, 50.8, 49.4; IR (neat, cm^{-1}): 3340, 3195, 2920, 1610, 1502, 1248, 1151, 779, 700; HRMS (APCI/ASAP, m/z): 376.4361 (calcd. $C_{22}H_{22}FN_3O_3$, 376.4359, $[M+H]^+$).

4.12.11 (*R*)-*N*-(1-(2-Fluorophenyl)ethyl)-6-(4-methoxyphenyl)furo[2,3-*d*]pyrimidin-4-amine (13a)

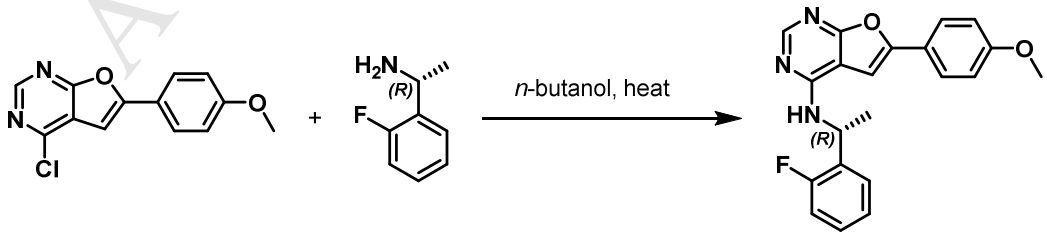

Compound **13a** was prepared as described in Section 4.10 starting with 4-chloro-6-(4-methoxyphenyl)furo[2,3-*d*]pyrimidine (**5a**) (200 mg, 0.77 mmol) and (*R*)-1-(2-fluorophenyl)ethan-1-amine (250 mg, 1.80 mmol). The reaction mixture was heated at 140

°C for 18 h. Column chromatography on silica-gel (*n*-pentane/EtOAc, 2/1, R_f = 0.75) yielded 186 mg (0.51 mmol, 66%) of **13a** as a pale yellow solid; mp 163 - 176 °C; HPLC purity: 97%, t_R = 25.2 min; $[\alpha]_D^{20}$ = -280.3 (c 1.01, DMSO); ^{1}H NMR (400 MHz, DMSO-d_6) δ: 8.30 (d, *J* = 7.7, 1H), 8.17 (s, 1H), 7.73 (d, *J* = 8.9, 2H), 7.49 -7.44 (m, 1H), 7.35 (s, 1H), 7.31-7.24 (m, 1H), 7.20-7.13 (m, 2H), 7.08 (d, *J* = 8.8, 2H), 5.69 – 5.65 (m, 1H), 3.82 (s, 3H), 1.55 (d, *J* = 7.0, 3H); ^{13}C NMR (100 MHz, DMSO-d_6) δ: 166.1, 160.2, 160.1 (d, *J* = 244.0), 156.3, 153.7, 151.1, 132.1 (d, *J* = 14.1), 129.1 (d, *J* = 8.2), 127.6 (d, *J* = 4.4), 126.2 (2C), 124.9 (d, *J* = 3.5), 122.3, 115.8 (d, *J* = 22.0), 115.2 (2C), 103.3, 97.6, 55.7, 44.3, 22.1; IR (neat, cm^{-1}): 3268, 2977, 2925, 2831, 1595, 1500, 1249, 1179, 1142, 1022, 828, 754; HRMS (APCI/ASAP, m/z): 364.1457 (calcd. $C_{21}H_{19}FN_3O_2$, 364.1461, $[M+H]^+$).

4.12.12 (*R*)-*N*-(1-(3-Fluorophenyl)ethyl)-6-(4-methoxyphenyl)furo[2,3-*d*]pyrimidin-4-amine (14a)

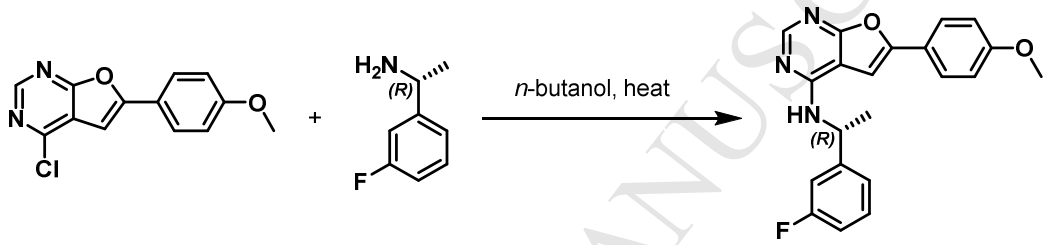

Compound **14a** was prepared as described in Section 4.10 starting with 4-chloro-6-(4-methoxyphenyl)furo[2,3-*d*]pyrimidine (**5a**) (200 mg, 0.77 mmol) and (*R*)-1-(3-fluorophenyl)ethan-1-amine (250 mg, 1.80 mmol). The reaction mixture was heated at 140 °C for 18 h. Column chromatography on silica-gel (*n*-pentane/EtOAc 2/1, R_f = 0.75) yielded 143 mg (0.390 mmol, 50%) of **14a** as a pale yellow solid; mp. 145 - 147 °C; HPLC purity: 96%, t_R = 26.8 min; $[\alpha]_D^{20}$= -252.3 (c 1.00, DMSO); ^{1}H NMR (400 MHz, DMSO-d_6) δ: 8.27 (d, *J* = 8.0, 1H), 8.18 (s, 1H), 7.73 (d, *J* = 8.8, 2H), 7.40 - 7.32 (m, 1H), 7.32 (s, 1H), 7.29 - 7.21 (m, 2H), 7.08 (d, *J* = 9.0, 2H), 7.06 - 7.00 (m, 1H), 5.47 – 5.43 (m, 1H), 3.81 (s, 3H), 1.54 (d, *J* = 7.0, 3H); ^{13}C NMR (100 MHz, DMSO-d_6) δ: 166.1, 162.7 (d, *J* = 243.7), 160.2, 156.4, 153.6, 151.1, 148.5(d, *J* = 6.6), 130.7 (d, *J* = 8.1), 126.2 (2C), 122.6 (d, *J* = 2.9), 122.3, 115.2 (2C), 113.9 (d, *J* = 21.3), 113.2 (d, *J* = 21.4), 103.2, 97.6, 55.8, 49.5, 23.1; IR (neat, cm^{-1}): 3440, 2961, 2923, 1598, 1502, 1251, 1177, 1145, 1021, 837, 786, 772, 693; HRMS (APCI/ASAP, m/z): 364.1461 (calcd. $C_{21}H_{19}FN_3O_2$, 364.1461, $[M+H]^+$).

4.12.13 (*R*)-*N*-(1-(4-Fluorophenyl)ethyl)-6-(4-methoxyphenyl)furo[2,3-*d*]pyrimidin-4-amine (15a)

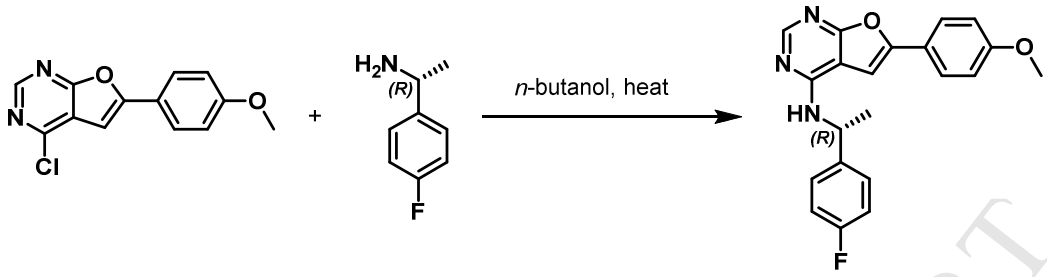

Compound **15a** was prepared as described in Section 4.10 starting with 4-chloro-6-(4-methoxyphenyl)furo[2,3-*d*]pyrimidine (**5a**) (300 mg, 1.15 mmol) and (*R*)-1-(4-fluorophenyl)ethan-1-amine (480 mg, 3.45 mmol). The reaction mixture was heated at 140 °C for 18 h. Column chromatography on silica-gel (EtOAc/*n*-pentane, 1/1, R_f = 0.75) yielded 103 mg (0.27 mmol, 39%) of **15a** as a yellow solid; mp 142-149 °C; HPLC purity: 97%, t_R = 27.3 min; $[\alpha]_D^{20}$ = -216.9 (c 1.00, DMSO); ^{1}H NMR (400 MHz, DMSO-d_6) δ: 8.24 (d, *J* = 7.9, 1H), 8.18 (s, 1H), 7.72 (d, *J* = 8.8, 2H), 7.49 - 7.43 (m, 2H), 7.31 (s, 1H), 7.13 (t, *J* = 8.8, 2H), 7.07 (d, *J* = 8.9, 2H), 5.47 – 5.43 (m, 1H), 3.81 (s, 3H), 1.56 (d, *J* = 7.1, 3H); ^{13}C NMR (100 MHz, DMSO-d_6) δ: 166.1, 161.5 (d, *J* = 241.9), 160.2, 159.9, 156.4, 153.7, 151.1, 141.4 (d, *J* = 3.1), 128.4 (d, *J* = 8.2, 2C), 126.2 (2C), 122.3, 115.4 (d, *J* = 20.9, 2C) 115.2 (2C), 103.3, 97.6, 55.8, 49.2, 23.1; IR (neat, cm^{-1}): 3381, 3273, 2966, 2919, 2358, 1610, 1579, 1501, 1252, 1174, 1023, 836, 769; HRMS (APCI/ASAP, m/z): 364.1456 (calcd. $C_{21}H_{19}FN_3O_2$, 364.1461, $[M+H]^+$).

4.12.14(R)-N-(1-Cyclohexylethyl)-6-(4-methoxyphenyl)furo[2,3-d]pyrimidin-4-amine (16a)

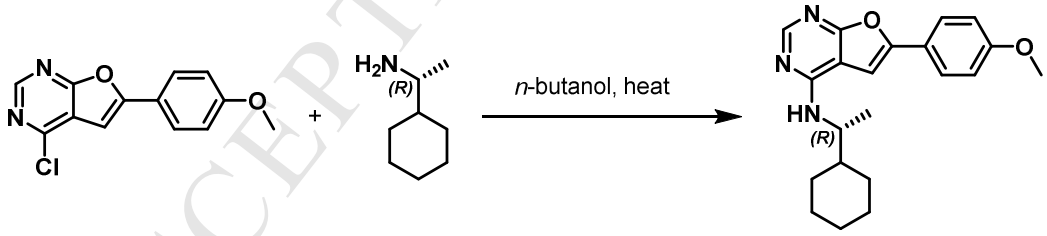

Compound **16a** was prepared as described in Section 4.10 starting with 4-chloro-6-(4-methoxyphenyl)furo[2,3-*d*]pyrimidine (**5a**) (299 mg, 1.12 mmol) and (*R*)-1-cyclohexylethan-1-amine (438 mg, 3.45 mmol). The reaction mixture was heated at 120 °C for 22 h. Column chromatography on silica-gel (*n*-pentane/EtOAc, 6/4, R_f = 0.40) yielded 374 mg (1.06 mmol, 92%) of **16a** as an off-white foam; mp 91 - 93 °C; HPLC purity: 99%, t_R = 32.1 min; $[\alpha]_D^{20}$ = -95.2 (c 1.00, DMSO); ^{1}H NMR (400 MHz, DMSO-d_6) δ: 8.18 (s, 1H), 7.71 - 7.70 (m, 2H), 7.59 - 7.57 (m, 1H), 7.29 (s, 1H), 7.08 - 7.06 (m, 2H), 4.22 - 4.17 (m, 1H), 3.81 (s, 3H), 1.80 - 1.67 (m, 4H), 1.62 - 1.60 (m, 1H), 1.51 - 1.44 (m, 1H), 1.21 - 1.09 (m, 6H), 1.04 - 0.98 (m, 2H); ^{13}C NMR (100 MHz, DMSO-d_6) δ:165.5, 159.6, 156.6, 153.3, 150.2, 125.6 (2C), 122.0, 114.7 (2C), 102.4, 97.2, 55.3, 50.0, 42.5, 29.3, 28.6, 26.0, 25.80, 25.75, 17.5; IR (neat, cm^{-1}):

3274, 2924, 2850, 1595, 1502, 1463, 1249, 1144, 1022, 830, 779; HRMS (APCI/ASAP, m/z): 352.2028 (calcd. $C_{21}H_{26}N_3O_2$, 352.2025, $[M+H]^+$).

4.12.15 (S)-2-((6-(4-Methoxyphenyl)furo[2,3-d]pyrimidin-4-yl)amino)propan-1-ol (17a)

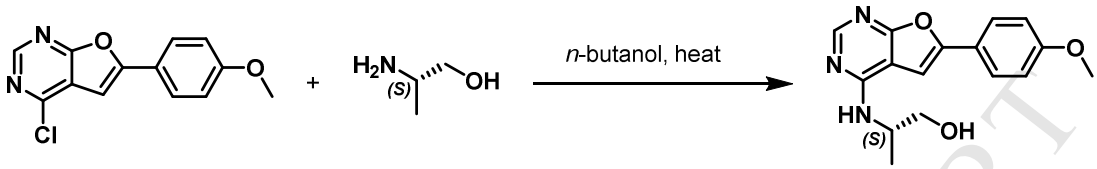

Compound **17a** was prepared as described in Section 4.10 starting with 4-chloro-6-(4-methoxyphenyl)furo[2,3-*d*]pyrimidine (**5a**) (300 mg, 1.15 mmol) and (*S*)-aminopropan-1-ol (260 mg, 3.45 mmol). The reaction mixture was heated at 120 °C for 24 h. Column chromatography on silica-gel (Et_2O/MeOH, 9/1, R_f = 0.43) yielded 317 mg (1.06 mmol, 92%) of **17a** as a pale foam; mp. 202 - 203 °C; HPLC purity: 99%, t_R = 18.2 min; $[\alpha]_D^{20}$ = -53.9 (c 1.02, DMSO); ^{1}H NMR (400 MHz, DMSO-d_6) δ: 8.21 (s, 1H), 7.72 - 7.70 (m, 2H), 7.60 - 7.58 (m, 1H), 7.28 (s, 1H), 7.09 - 7.05 (m, 2H), 4.82 (t, *J* = 5.6, 1H), 4.30 (pent, *J* = 6.6, 1H), 3.81 (s, 3H), 3.57 - 3.52 (m, 1H), 3.44 - 3.38 (m, 1H), 1.21 (d, *J* = 6.6, 3H); ^{13}C NMR (100 MHz, DMSO-d_6) δ: 165.6, 159.7, 156.6, 153.3, 150.3, 125.7 (2C), 122.0, 114.7 (2C), 102.6, 97.3, 64.3, 55.3, 48.0, 17.3; IR (neat, cm^{-1}): 3247, 3164, 2925, 1612, 1500, 1251, 1153, 1022, 784; HRMS (APCI/ASAP, m/z): 300.1350 (calcd. $C_{16}H_{18}N_3O_3$, 300.1348, $[M+H]^+$).

4.12.16 (*S*)-6-(4-Methoxyphenyl)-*N*-(1-phenylethyl)furo[2,3-*d*]pyrimidin-4-amine (18a)

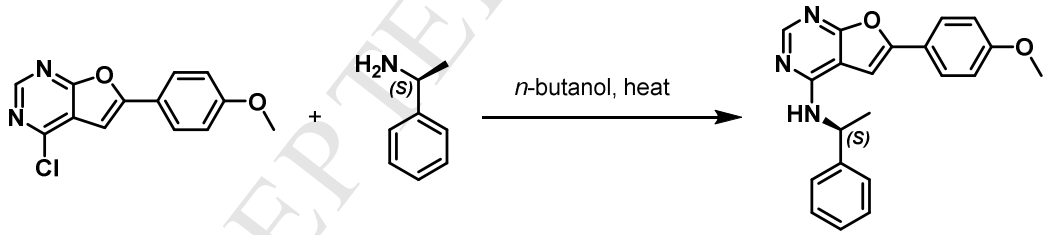

Compound **18a** was prepared as described in Section 4.10 starting with 4-chloro-6-(4-methoxyphenyl)furo[2,3-*d*]pyrimidine (**5a**) (300 mg, 1.15 mmol) and (*S*)-1-phenylethan-1-amine (418 mg, 3.46 mmol). The reaction mixture was heated at 140 °C for 17 h. Column chromatography on silica-gel (*n*-pentane/EtOAc 2/1, R_f = 0.41) yielded 321 mg (0.930 mmol, 81%) of **18a** as a pale yellow solid; mp. 128 - 129 °C; HPLC purity: 96%, t_R = 25.2 min; $[\alpha]_D^{20}$ = 270.4 (c 0.99, DMSO); ^{1}H NMR (400 MHz, DMSO-d_6) δ: 8.26 - 8.24 (m, 1H), 8.17 (s, 1H), 7.74 - 7.70 (m, 2H), 7.44 - 7.41 (m, 2H), 7.35 - 7.31 (m, 3H), 7.23 - 7.20 (m, 1H), 7.10 - 7.07 (m, 2H), 5.48 - 5.42 (m, 1H), 3.82 (s, 3H), 1.55 (d, *J* = 7.0, 3H). ^{13}C NMR (100 MHz, DMSO-d_6) δ: 166.1, 160.2, 156.5, 153.7, 151.0, 145.3, 128.8 (2C), 127.1, 126.5 (2C), 126.2 (2C), 122.4, 115.2 (2C), 103.2, 97.7, 55.8, 49.7, 23.2; IR (neat, cm^{-1}): 3264, 2970, 2930, 2833, 1593, 1503, 1249, 1172, 1135, 1021, 831, 777, 697; HRMS (APCI/ASAP, m/z): 346.1551 (calcd. $C_{21}H_{20}N_3O_2$, 346.1556, $[M+H]^+$).

4.13 Docking and dynamics

The X-ray crystal structures of the protein 2J6M (Wild-type EGFR) were prepared using the protein preparation wizard, which is part of the Maestro software package (Maestro, v8.5; Schrödinger, LLC, New York, NY, USA) using the OPLS-3 force field. The resulting protein structures were used in the following docking study. Ligands were drawn using ChemBioDraw (ChemBioDraw Ultra 13.0, CambridgeSoft, PerkinElmer) or the Maestro 2D Sketcher tool and were prepared using LigPrep2.2 (LigPrep, v2.2; Schrödinger, LLC). For the computational investigation of the receptor-inhibitor structures, the energy minimized structures of 2J6M and ligands were subsequently docked using induced-fit docking (IFD) of Schrödinger [26-28]. Briefly this was achieved by doing an initial docking for each ligand using Glide and a softened potential (van der Waals radii scaling). A maximum of 20 poses per ligand were retained. Side-chain prediction for each protein-ligand complex on residues within 5 Å of the ligands were then calculated using Prime and the same set of ligands and residues were subsequently minimized using Prime minimization. Finally, the ligands within a specified energy from the lowest-energy structure (30 kcal/mol) were redocked on the modified receptor structure using default Glide settings.The resulting docked poses were analysed using Glide pose viewer tool. For dynamic simulation, the best poses from docking were used as starting points when building the model systems Dynamic simulations were conducted for 10 ns simulation time using Maestros Desmond suite [29], the OPLS-3 force field and a TIP4P solvent model. Briefly, this was performed by putting the docked protein-ligand complex inside a minimized solvent box and adding ions (Na^+ or Cl^-) in order to have an electrical neutral system. Finally NaCl was added to a total concentration of 0.15 M, which is approximately the physiological concentration of monovalent ions. This gave normally a system of approximately 39 000 atoms. Molecular dynamics were then calculated on these systems using the isothermal-isobaric (NPT) ensemble at 300K and 1.01325 bar. Trajectory analysis were performed using Desmond´s Simulation Interactions Diagram tool and all the graphical pictures were made using Maestro or Pymol (The PyMOL Molecular Graphics System, Version 1.8 Schrödinger, LLC).

Acknowledgements

Susana Villa Gonzalez is thanked for the HRMS experiments. Sandra Lange and Martin Varek are acknowledged for performing some of the reactions. Prof. Dr. Justus Duyster and Dr. Nikolas von Bubnoff, Technical University of Munich, Munich, Germany kindly provided EGFR Ba/F3 cells. The research was financially supported by Anders Jahres foundation and Technology Transfer Office (TTO-NTNU Trondheim). NOTUR is acknowledged for CPU-time.

Author Contributions

The synthetic work was performed by J. Han, S.J. Kaspersen and S. Nervik. Molecular docking and dynamics performed by E. Sundby. Cellular experiments were performed by K. Nørsett. J. Han and B. Hoff planed the work and wrote the paper.

Supplementary Material: This file contains *in vitro* kinase data with standard deviations, kinase selectivity data, EGFR-ligand interactions maps following dynamics and selected NMR spectra. The material is available free of charge.

5.0 References

[1] Y. Yarden, G. Pines, The ERBB network: at last, cancer therapy meets systems biology, Nat. Rev. Cancer, 12 (2012) 553-563.
[2] N. Cook, K.K. Frese, M. Moore, Assessing the role of the EGF receptor in the development and progression of pancreatic cancer, Gastrointest. Cancer: Targets Ther, 4 (2014) 23-37.
[3] D.R. Siwak, M. Carey, B.T. Hennessy, C.T. Nguyen, M.J. McGahren Murray, L. Nolden, G.B. Mills, Targeting the epidermal growth factor receptor in epithelial ovarian cancer: current knowledge and future challenges, J Oncol, 2010 (2010) Article ID 568938.
[4] T. Zellweger, C. Ninck, M. Bloch, M. Mirlacher, P.A. Koivisto, H.J. Helin, M.J. Mihatsch, T.C. Gasser, L. Bubendorf, Expression patterns of potential therapeutic targets in prostate cancer, Int. J. Cancer, 113 (2005) 619-628.
[5] C. Kersten, M. Grønlie Cameron, S. Mjåland, Epithelial growth factor receptor (EGFR)-inhibition for relief of neuropathic pain—A case series, Scand. J. Pain, 4 (2013) 3-7.
[6] C. Kersten, M.G. Cameron, S. Mjaland, Epidermal growth factor receptor (EGFR) targeted therapy for treatment of neurological disorders, 2013005108, 2013.
[7] S.N. Li, H.Q. Li, Epidermal growth factor receptor inhibitors: a patent review (2010 - present), Expert Opin. Ther. Pat, 24 (2014) 309-321.
[8] Y.J. Liu, C.M. Zhang, Z.P. Liu, Recent developments of small molecule EGFR inhibitors based on the quinazoline core scaffolds, Anti-Cancer Agents Med. Chem, 12 (2012) 391-406.
[9] S. Bugge, A.F. Buene, N. Jurisch-Yaksi, I.U. Moen, E.M. Skjoensfjell, E. Sundby, B.H. Hoff, Extended structure-activity study of thienopyrimidine-based EGFR inhibitors with evaluation of drug-like properties, Eur. J. Med. Chem., 107 (2016) 255-274.
[10] S. Bugge, S.J. Kaspersen, S. Larsen, U. Nonstad, G. Bjørkøy, E. Sundby, B.H. Hoff, Structure-activity study leading to identification of a highly active thienopyrimidine based EGFR inhibitor, Eur. J. Med. Chem, 75 (2014) 354-374.
[11] P. Traxler, P.R. Allegrini, R. Brandt, J. Brueggen, R. Cozens, D. Fabbro, K. Grosios, H.A. Lane, P. McSheehy, J. Mestan, T. Meyer, C. Tang, M. Wartmann, J. Wood, G. Caravatti, AEE788: A Dual Family Epidermal Growth Factor Receptor/ErbB2 and Vascular Endothelial Growth Factor Receptor Tyrosine Kinase Inhibitor with Antitumor and Antiangiogenic Activity, Cancer Res, 64 (2004) 4931-4941.
[12] G. Caravatti, J. Bruggen, E. Buchdunger, R. Cozens, P. Furet, N. Lydon, T. O'Reilly, P. Traxler, Pyrrolo[2,3-d]pyrimidine and pyrazolo[3,4-d]pyrimidine derivatives as selective inhibitors of the EGF receptor tyrosine kinase, ACS Symposium Series, 796 (2001) 231-244.
[13] S.J. Kaspersen, J. Han, K.G. Nørsett, L. Rydså, E.B. Kjøbli, S., G. Bjørkøy, E. Sundby, B.H. Hoff, Identification of new 4-*N*-substituted 6-aryl-7*H*-pyrrolo[2,3-*d*]pyrimidine-4-amines as highly potent EGFR-TK inhibitors with Src-family activity, Eur. J. Pharm. Sci, 59 (2014) 69-82.
[14] M.R. Eno, M.D. Cameron, Gauging Reactive Metabolites in Drug-Induced Toxicity, Curr. Med. Chem., 22 (2015) 465-489.
[15] P.A. Harris, D. Bandyopadhyay, S.B. Berger, N. Campobasso, C.A. Capriotti, J.A. Cox, L. Dare, J.N. Finger, S.J. Hoffman, K.M. Kahler, R. Lehr, J.D. Lich, R. Nagilla, R.T. Nolte, M.T. Ouellette, C.S. Pao, M.C. Schaeffer, A. Smallwood, H.H. Sun, B.A. Swift, R.D. Totoritis, P. Ward, R.W. Marquis, J. Bertin, P.J. Gough, Discovery of Small Molecule RIP1 Kinase Inhibitors for the Treatment of Pathologies Associated with Necroptosis, ACS Med. Chem. Lett, 4 (2013) 1238-1243.

[16] X. Zhang, S. Raghavan, M. Ihnat, J.E. Thorpe, B.C. Disch, A. Bastian, L.C. Bailey-Downs, N.F. Dybdal-Hargreaves, C.C. Rohena, E. Hamel, S.L. Mooberry, A. Gangjee, The design and discovery of water soluble 4-substituted-2,6-dimethylfuro[2,3-d]pyrimidines as multitargeted receptor tyrosine kinase inhibitors and microtubule targeting antitumor agents, Bioorg. Med. Chem, 22 (2014) 3753-3772.
[17] H.Y. Shiao, M.S. Coumar, C.W. Chang, Y.Y. Ke, Y.H. Chi, C.Y. Chu, H.Y. Sun, C.H. Chen, W.H. Lin, K.S. Fung, P.C. Kuo, C.T. Huang, K.Y. Chang, C.T. Lu, J.T.A. Hsu, C.T. Chen, W.T. Jiaang, Y.S. Chao, H.P. Hsieh, Optimization of Ligand and Lipophilic Efficiency To Identify an in Vivo Active Furano-Pyrimidine Aurora Kinase Inhibitor, J. Med. Chem, 56 (2013) 5247-5260.
[18] Y. Miyazaki, S. Matsunaga, J. Tang, Y. Maeda, M. Nakano, R.J. Philippe, M. Shibahara, W. Liu, H. Sato, L. Wang, R.T. Nolte, Novel 4-aminofuro[2,3-d]pyrimidines as Tie-2 and VEGFR2 dual inhibitors, Bioorg. Med. Chem. Lett, 15 (2005) 2203-2207.
[19] A. Martin-Kohler, J. Widmer, G. Bold, T. Meyer, U. Sequin, P. Traxler, Furo[2,3-d]pyrimidines and oxazolo[5,4-d]pyrimidines as inhibitors of receptor tyrosine kinases (RTK), Helv. Chim. Acta, 87 (2004) 956-975.
[20] Y.H. Peng, H.Y. Shiao, C.H. Tu, P.M. Liu, J.T.-A. Hsu, P.K. Amancha, J.S. Wu, M.S. Coumar, C.H. Chen, S.Y. Wang, W.H. Lin, H.Y. Sun, Y.S. Chao, P.C. Lyu, H.P. Hsieh, S.Y. Wu, Protein Kinase Inhibitor Design by Targeting the Asp-Phe-Gly (DFG) Motif: The Role of the DFG Motif in the Design of Epidermal Growth Factor Receptor Inhibitors, J. Med. Chem, 56 (2013) 3889-3903.
[21] S. Bugge, I.U. Moen, K.O. Kragseth Sylte, E. Sundby, B.H. Hoff, Truncated structures used in search for new lead compounds and in a retrospective analysis of thienopyrimidine-based EGFR inhibitors, Eur. J. Med. Chem, 94 (2015) 175-194.
[22] S.J. Kaspersen, C. Sørum, V. Willassen, E. Fuglseth, E. Kjøbli, G. Bjørkøy, E. Sundby, B.H. Hoff, Synthesis and in vitro EGFR (ErbB1) tyrosine kinase inhibitory activity of 4-N-substituted 6-aryl-7H-pyrrolo[2,3-d]pyrimidine-4-amines, Eur. J. Med. Chem, 46 (2011) 6002-6014.
[23] E. Sundby, J. Han, S.J. Kaspersen, B.H. Hoff, *In vitro* baselining of new pyrrolopyrimidine EGFR-TK inhibitors with Erlotinib, Eur. J. Pharm. Sci, 80 (2015) 56-65.
[24] S. Koide, S.S. Sidhu, The Importance of Being Tyrosine: Lessons in Molecular Recognition from Minimalist Synthetic Binding Proteins, ACS Chem. Biol., 4 (2009) 325-334.
[25] S. Gronowitz, C. Westerlund, A.B. Hornfeldt, Synthetic utility of heteroaromatic azido compounds. I. Preparation and reduction of some 3-azido-2-substituted furans, thiophenes, and selenophenes, Acta Chem. Scand. , Ser. B, B29 (1975) 224-232.
[26] Induced fit docking protocol 2013-3, Glide version 6.1, Prime version 3.4, Schrödinger, LLC, New York, NY,, in, 2013.
[27] W. Sherman, H.S. Beard, R. Farid, Use of an induced fit receptor structure in virtual screening, Chem. Biol. Drug Des, 67 (2006) 83-84.
[28] W. Sherman, T. Day, M.P. Jacobson, R.A. Friesner, R. Farid, Novel Procedure for Modeling Ligand/Receptor Induced Fit Effects, J. Med. Chem, 49 (2006) 534-553.
[29] v. Desmond Molecular Dynamics System, D. E. Shaw Research, New York, NY, 2014. Maestro-Desmond Interoperability Tools, version 3.9, Schrödinger, New York, NY, 2014., in.
[30] C.H. Wu, M.S. Coumar, C.Y. Chu, W.H. Lin, Y.R. Chen, C.T. Chen, H.Y. Shiao, S. Rafi, S.Y. Wang, H. Hsu, C.H. Chen, C.Y. Chang, T.Y. Chang, T.W. Lien, M.Y. Fang, K.C. Yeh, C.P. Chen, T.K. Yeh, S.H. Hsieh, J.T.-A. Hsu, C.C. Liao, Y.S. Chao, H.P. Hsieh, Design and synthesis of tetrahydropyridothieno[2,3-d]pyrimidine scaffold based epidermal growth factor receptor (EGFR) kinase inhibitors: The role of side chain chirality and Michael acceptor group for maximal potency, J. Med. Chem, 53 (2010) 7316-7326.
[31] P. Hermet, J.L. Bantignies, J.P. Lere-Porte, F. Serein-Spirau, Far-infrared spectroscopy investigation of sulfur-oxygen interactions in π-conjugated oligomers, Chem. Phys. Lett., 535 (2012) 116-119.
[32] M.K. Si, R. Lo, B. Ganguly, The origin and magnitude of intramolecular quasi-cyclic S···O and S···S interactions revisited: A computational study, Chem. Phys. Lett., 631-632 (2015) 6-11.

[33] P.P. Graczyk, Gini Coefficient: A New Way To Express Selectivity of Kinase Inhibitors against a Family of Kinases, J. Med. Chem, 50 (2007) 5773-5779.
[34] S.J. Coniglio, E. Eugenin, K. Dobrenis, E.R. Stanley, B.L. West, M.H. Symons, J.E. Segall, Microglial stimulation of glioblastoma invasion involves epidermal growth factor receptor (EGFR) and colony stimulating factor 1 receptor (CSF-1R) signaling, Mol. Med. , 18 (2012) 519-527.
[35] R.K. Kancha, N. von Bubnoff, C. Peschel, J. Duyster, Functional Analysis of Epidermal Growth Factor Receptor (EGFR) Mutations and Potential Implications for EGFR Targeted Therapy, Clin. Cancer Res, 15 (2009) 460-467.
[36] B.A. Pollok, B.D. Hamman, S.M. Rodems, L.R. Makings, Optical probes and assays, WO 2000066766 A1, 2000.
[37] S.J. Haycock-Lewandowski, A. Wilder, J. Ahman, Development of a Bulk Enabling Route to Maraviroc (UK-427,857), a CCR-5 Receptor Antagonist, Org. Process Res. Dev, 12 (2008) 1094-1103.
[38] G. Cardillo, L. Gentilucci, A. Tolomelli, C. Tomasini, A Stereoselective Synthesis of (2R,3S)-N-Benzoylphenylisoserine Methyl Ester, J. Org. Chem., 63 (1998) 2351-2353.
[39] E. Choi, Y. Kim, Y. Ahn, J. Park, M.J. Kim, Highly enantioselective enzymatic resolution of aromatic β-amino acid amides with Pd-catalyzed racemization, Tetrahedron: Asymmetry, 24 (2013) 1449-1452.
[40] V. Chhiba, M.L. Bode, K. Mathiba, W. Kwezi, D. Brady, Enantioselective biocatalytic hydrolysis of β-aminonitriles to β-amino-amides using *Rhodococcus rhodochrous* ATCC BAA-870, J. Mol. Catal. B: Enzym, 76 (2012) 68-74.
[41] M. Nakano, Preparation of N-(furo[2,3-d]pyrimidin-4-yl) amides as GSK-3 inhibitors, WO 2005061516, 2005.
[42] F.M. Abdelrazek, H.M. Hassaneen, E.M. Nassar, A. Jager, Phenacyl bromides revisited: Facile synthesis of some new pyrazoles, pyridazines, and their fused derivatives, J. Heterocycl. Chem, 51 (2014) 475-481.
[43] M.S. Coumar, M.T. Tsai, C.Y. Chu, B.J. Uang, W.H. Lin, C.Y. Chang, T.Y. Chang, J.S. Leou, C.H. Teng, J.S. Wu, M.Y. Fang, C.H. Chen, J.T.-A. Hsu, S.Y. Wu, Y.S. Chao, H.P. Hsieh, Identification, SAR Studies, and X-ray Co-crystallographic Analysis of a Novel Furanopyrimidine Aurora Kinase A Inhibitor, ChemMedChem, 5 (2010) 255-267.
[44] T. Matsuda, K. Yamagata, Y. Tomioka, M. Yamazaki, Studies on heterocyclic enaminonitriles. VI. Synthesis of 2-amino-3-cyano-4,5-dihydrofurans, Chem. Pharm. Bull, 33 (1985) 937-943.
[45] M. Bakavoli, M. Rahimizadeh, Z. Gordi, One-pot synthesis of substituted 2-amino-3-furonitriles, J. Chem. Res, (2008) 564-565.
[46] B.S. Yang, K.M. Yang, H.J. Kim, I.S. Park, S.D. Park, J.H. Lee, H.M. Kwon, B.Y. Woo, Preparation of furo[2,3-d]pyrimidines as inhibitors of DDR2 (discoidin domain receptor 2) tyrosine kinase, WO 2005092896, 2005.

Figures and schemes:

Figure 1. Examples of furopyrimidines previously evaluated as kinase inhibitors.

Figure 2. Structure of thieno-, pyrrolo- and the investigated furopyrimidines.

Figure 3. Effect of variation of the 6-aryl group on the EGFR IC_{50} value (nM). (The supplementary material file contain information on number of measurements and standard deviations).

Figure 4. EGFR ligand interactions as identified by docking and molecular dynamics for **6j**. (The 2D representation of the 3-dimentional image wrongly shows the position of the *ortho* substituents.) Docking and dynamics showed these to have an anti-relationship to the furan oxygen.

Figure 5. IC_{50} curves with error bars of **6b** (20 data points), **6j** (20 data points), **6l** (40 data points) and **6n** (40 data points).

Figure 6. EGFR ligand interactions as identified by docking and molecular dynamics for **6l** (docking score: -12.47).

Figure 7. Effect of varying the 4-amino group in the a-series on the EGFR IC_{50} values. (The Supplementary Material file contain information on number of measurements and standard deviations).

Figure 8. Attempts to improve potency by combining activity inducing fragments.

Figure 9. Structure activity relationship data obtained in this study.

Figure 10. Effect of scaffold hopping: EGFR activity of furo- vs. thieno- and pyrrolopyrimidines. Numbering corresponds to the structure of the furopyrimidines. The comparison contains data for 18 furopyrimidines, 18 pyrrolopyrimidines [13, 22] and 10 thienopyrimidines [9, 10].

Figure 11. Overlay of the docked structures **6j** and the corresponding thienopyrimidine analogue.

Figure 12. Kinase inhibition profile of **6l**, **6n** and Erlotinib sorted by the activity of **6n.**

Figure 13. Cell proliferation study of compounds **6l** and **6n** compared to Erlotinib using Ba/F3-EGFR^{L858R} cells. Each data point shown is the average of three independent replicates. IC_{50}: Erlotinib: 87±5; **6l**: 217±24, **6n**: 196±6.

Scheme 1. Synthetic route to the target compounds **6-18**.

Scheme 2. Post modifications on derivatives **6a**, **6d**, **6f** and **6g**.

Research highlights

- SAR on furopyrimidine based EGFR inhibitors (29 ex.)
- Stereochemistry of uttermost importance for activity
- Two highly active derivatives discovered
- Profiling in a panel of 50 kinases
- The furopyrimidine scaffold is highly useful for making new EGFR inhibitors.